Copyright Warning & Restrictions

The copyright law of the United States (Title 17, United States Code) governs the making of photocopies or other reproductions of copyrighted material.

Under certain conditions specified in the law, libraries and archives are authorized to furnish a photocopy or other reproduction. One of these specified conditions is that the photocopy or reproduction is not to be "used for any purpose other than private study, scholarship, or research." If a, user makes a request for, or later uses, a photocopy or reproduction for purposes in excess of "fair use" that user may be liable for copyright infringement,

This institution reserves the right to refuse to accept a copying order if, in its judgment, fulfillment of the order would involve violation of copyright law.

Please Note: The author retains the copyright while the New Jersey Institute of Technology reserves the right to distribute this thesis or dissertation

Printing note: If you do not wish to print this page, then select "Pages from: first page # to: last page #" on the print dialog screen

ABSTRACT

Entrance Effects For Short Catalytic Combustion Monoliths

by
Dong Dai

Catalytic combustion/incineration is becoming increasingly important in modern industrial processes. This thesis work investigates the importance of heat and mass transfer entrance effects in short catalytic combustion monoliths, and includes these effects in an engineering model. Consideration is limited to laminar-flow heat and mass transfer in a circular tube, in which Prandtl number is close to unity, as is the case for air. Thermal, mass and velocity boundary layer growths are considered with inlet conditions assumed uniform at a monolith bed entrance. Conservation equations are solved assuming laminar, steady-state flow, with constant wall temperature, and negligible axial diffusion of heat and mass. The results compare fuel conversion with and without consideration of entrance effects. At low inlet temperature, inclusion of entry effects results in higher fuel conversion that due to increased mass transport. However, for high inlet temperature, the entry length effects make a negative contribution to surface temperature due to increased heat transport, thus decreasing the conversion rate. Finally, turbulent flow conditions are discussed with the conclusion of decreased importance of the entrance length region.

ENTRANCE EFFECTS FOR SHORT CATALYTIC COMBUSTION MONOLITHS

by

Dong Dai

A Thesis
Submitted to the Faculty of
New Jersey Institute of Technology
in Partial Fulfillment of the Requirements for the Degree of
Master of Science

Department of Mechanical Engineering

January, 1993

APPROVAL PAGE

Entrance Effects For Short Catalytic Combustion Monoliths

Dong Dai

Dr. Anthony E. Cerkanowicz, Thesis Adviser
Associate Professor of Mechanical Engineering, NJIT

Dr. Rong-Yaw Chen, Committee Member
Associate Graduate Chairperson and Professor of Mechanical Engineering, NJIT

Dr. Robert P. Kirchner, Committee Member
Professor of Mechanical Engineering, NJIT

BIOGRAPHICAL SKETCH

Author: Dong Dai

Degree: Master of Science in Mechanical Engineering

Date: January, 1993

Undergraduate and Graduate Education:

- Master of Science in Mechanical Engineering,
  New Jersey Institute of Technology, Newark, New Jersey, 1993
- Bachelor of Science in Chemical Engineering Mechanics,
  East China University of Chemical Technology, Shanghai, People's Republic of China, 1982

Major: Mechanical Engineering

This thesis is dedicated to
my dear parents and my dear wife

ACKNOWLEDGMENT

The author would like to acknowledge his great indebtedness to Dr. Anthony E. Cerkanowicz who taught me all I profess to know about my research work, and spent a lot of invaluable time to guide my thesis work, as well as grant the opportunity for my research assistantship.

Special thanks are also due to Dr. Rong-Yaw Chen and Dr. Robert P. Kirchner for serving as members of the thesis committee.

My sincere appreciation is extended to Dr. Henry Shaw for the timely help and suggestions.

TABLE OF CONTENTS

LIST OF TABLES

LIST OF FIGURES

LIST OF NOMENCLATURE

Symbol	Definition	Unit
English Letter Symbols		
c	specific heat	J/(kg K)
C	molar density of species	kmol /m^3
D	tube diameter	m
D_{AB}	molecular diffusion coefficient	m^2/s
G	mass flux	kg/(s m^2)
h	unit conductance for convection heat transfer	W/(m^2K)
hm	unit mass transfer coefficient	m/s
k	unit thermal conductivity	W/(m K)
L	tube length	m
$q"_w$	heat flux	W/m^2
r	tube-radius position	m
T	temperature	^oC or ^oK
Tm	mixed mean fluid temperature	^oC or ^oK
Tw	wall temperature	^oC or ^oK
T_∞	ambient temperature	^oC or ^oK
v	fluid velocity	m/s
v_r	component of fluid velocity in radial direction	m/s
x	distance measured from the tube entrance	m
x_e	tube entry length	m
Greek Letter Symbols		
ρ	fluid density	kg/m^3
μ	fluid viscosity	N s/m^2
α	thermal diffusivity, $=k/\rho c_p$	m^2/s

υ	momentum diffusivity, $=\mu/\rho$	m^2/s

Nondimensional Groups

Gz	Gretz number, $=Re\ Pr/(x/D)$
Nu	Nusselt number, $=h\ D/k_{fluid}$
Nux	local Nusselt number, $=h\ x/k_{fluid}$
Num	mean Nusselt number, defined by equation (3.9)
Nu_∞	fully developed Nusselt number, defined by equation (5.2)
Pe	Peclet number, $=Re\ Pr$
Pr	Prandtl number, $=\mu\ c_p/k$
Re	Reynolds number based on tube diameter, $=\rho\ v\ D/\mu$
Sc	Schmidt number, $=\upsilon/D_{AB}$
Sh	Sherwood number, $=hm\ D/D_{AB}$

Subscripts

e	entrance
F	fuel
g	gas
m	mixed mean value
p	constant pressure
r	radial direction
s	substrate surface
w	wall value
x	local value
∞	ambient/infinite distance
*	dimensionless variable

HFD	hydrodynamically fully developed
TFD	thermally fully developed
CFD	concentration fully developed

CHAPTER ONE
INTRODUCTION

Catalytic oxidation involves the use of surface deposited catalysts to promote oxidation of fuels or low concentration contaminants. Catalytic combustion of primary fuels is directed to achieving significant energy release, typically for power production. Catalytic incineration refers to the oxidative destruction of undesirable contaminants, typically at low concentration. Both have the potential to assume an important role in modern industrial processes to control emissions to the environment. One advantage of using catalytic combustion/incineration is low temperature ignition of oxidation reactions. For catalytic incinerators this considerably reduces both the energy requirements (need for auxiliary fuel) for stable combustion and the space for equipment. For catalytic combustion systems, the need for high temperature combustion initiation and stabilization regions are avoided thereby reducing environmental emissions. Another advantage is the ability to control the selectivity of waste compound destruction and the efficiency of fuel consumption. Typically, monoliths (or honeycombs) and packed beds are the two major types of arrangements for the catalytic support (bed) structure. High flow rate, low pressure drop systems favor the monolith configuration.

As part of an NJIT research program funded by the Hazardous Substance Research Center, an engineering model of the catalytic combustion/incineration process has continued to be developed based on the early work of Dr. Cerkanowicz [1]. Both the monolith and packed bed support structures are considered in this model. Excellent agreement

between model predictions and experimental catalytic combustion data has been demonstrated.

The objective of this thesis work is to demonstrate the importance of heat and mass transfer entrance effects in short catalytic combustion monoliths, and to include these effects in the engineering model. Consideration is limited to laminar-flow heat and mass transfer in a circular tube. Since air is the primary fluid of interest, Prandtl number near unity will be considered, with concentration, velocity, and temperature uniform at the tube entrance. Entrance length effects are expected to be particularly important when multiple spaced-apart reaction segments are employed.

The physical and chemical assumption of the model and the governing equations are addressed in chapter two. Heat and mass transfer in catalytic combustion monoliths can be modeled as heat and mass transport in constant diameter tubes representative of individual channels within the monolith. The transfer coefficients in the model were previously treated as constant along the tube length, with fully established velocity and temperature profiles assumed. This assumption will be correct only if the tube length, or the length of monolith, is long compared with the channel diameter. In many catalytic combustion applications, the bed length is short and consequently, the idealization of constant transport coefficients may seriously restrict the usefulness of the solution. Chapter three presents considerations of entry length heat and mass transfer, and the relevant equations describing the variation of heat transfer coefficient with distance from the channel entrance. Using a typical set of inlet parameters for a catalytic combustion reactor, chapter four presents results comparing fuel conversion computations with and without consideration of entry length

effects. The importance of properly including entry length considerations in modeling and the behavior of catalytic reactions are clearly developed. Chapter five presents the influence of flow turbulence. Summary conclusions are presented in chapter six.

CHAPTER TWO
CATALYTIC COMBUSTION MODEL

2.1 Physical and Chemical Assumptions of the Model

Figure 2.1 depicts the processes modeled in catalytic combustion. The flow is assumed to be steady-state, one-dimensional, plug flow. For flow through monoliths with non-circular channels, an equivalent channel diameter, hydraulic diameter, is defined. The incoming reactant mixture flow must accelerate in passing from the open area in front of the bed segment into the restricted opening of the bed segment. Mass and atom conservation equations and energy conservation equations (surface and gas phase) are written for the fluid flow, which is assumed to be "fuel" lean.

Radial diffusion of the fuel from the gas phase to the catalytic surface is a critical part of model development since the reactants reach the catalytic surface by this mechanism. For engineering design purposes, however, a detailed description of the radial concentration gradients for the reactants is not necessary. The use of transport correlations (heat and mass) provides sufficient radial transport information. Therefore, gas phase concentrations are assumed to be "mixing-cup" or cross-sectional average concentrations. Axial diffusion has been neglected in the model because of the sufficiently high reactant mixture velocity throughout the channel length. For the transport correlations, the description of an average heat transfer coefficient, taken as constant over the length of the catalytic surface area, was assumed in the previous version of the model. Modification of the heat transfer coefficient by considering axial variation due to entrance effects is a major object of this thesis work. The detailed

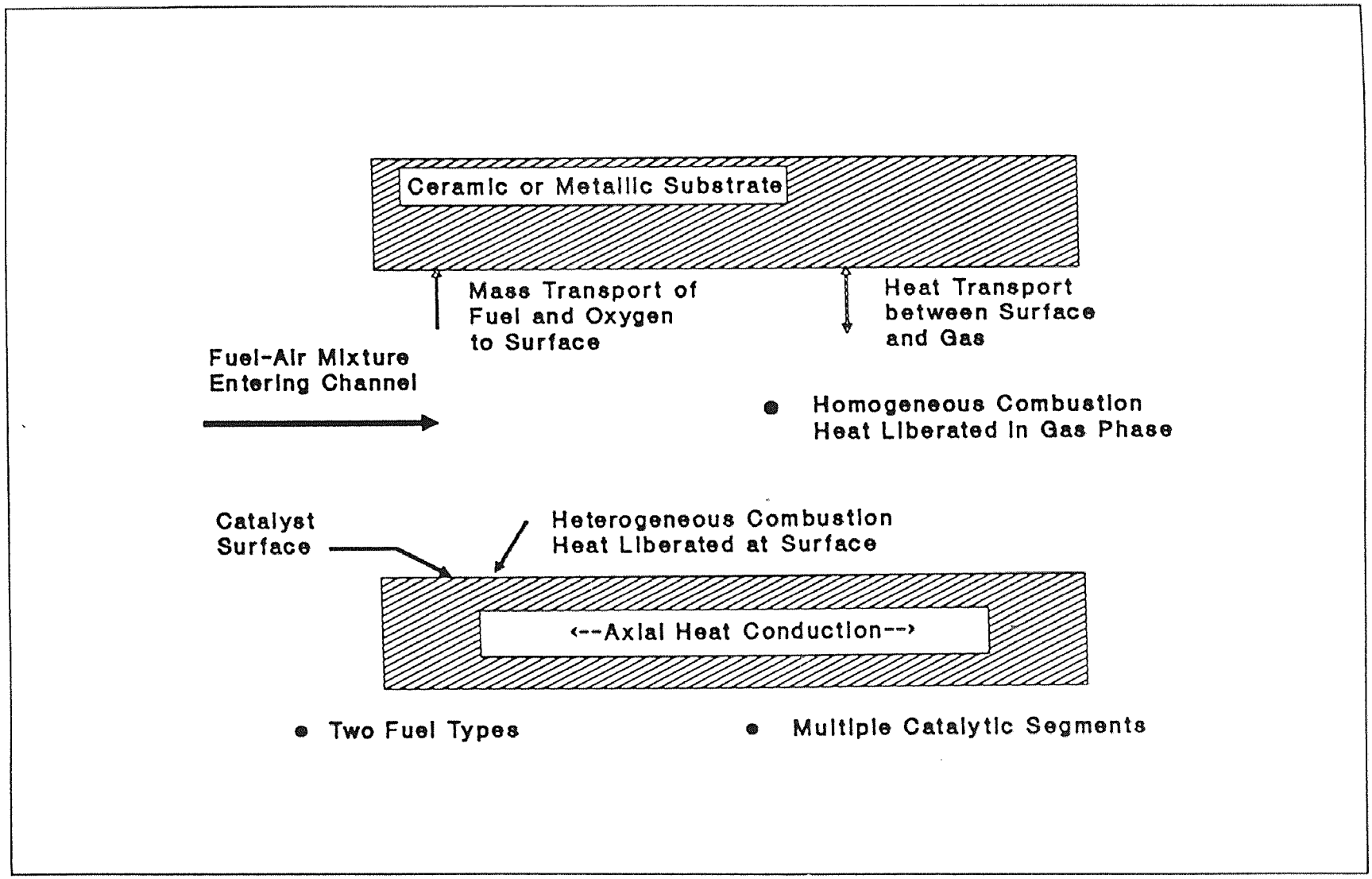

Figure 2.1 Chemical and Physical Processes Modeled in Catalytic Combustion

description of entrance effects will be provided in chapter three. Mass transport is modeled by using the analogy relating mass transport to heat transport as will be discussed in the same chapter.

Catalytic surface reaction is modeled by assuming a one-step (reactants to products), Arrhenious behavior. The dependence on the surface concentrations is taken to be first order in "fuel" (or reactant species) and zero order in the oxidizer. The later condition is particularly valid for fuel lean (excess air) conditions which describe the majority of current catalytic combustion applications. Heat of reaction liberated on the surface is conducted by the substrate in the axial direction and convected radially into gas phase. Additional consumption of reactants and heat release can occur in the gas phase by homogeneous reaction which is also modeled using one-step Arrhenious kinetics but with variable reactant orders. Each channel and its associated substrate material is represented as an adiabatic system, that is no heat loss to the surrounding environment, with the total heat release ultimately appearing in the exit gas flow.

2.2 Equations and Solving Methods Used in the Model

The equations used in the model include: the gas phase fuel species balance equation which relates the fuel convected axially, the fuel consumed in gas phase reaction, and fuel diffusion to the surface. On the surface, the fuel species balance relates the fuel diffusion to the surface and the fuel consumed in surface reactions. Fuel desorption is not considered to be a rate-limiting step. Conservation of energy in the gas phase relates energy convected axially, energy convected from the catalytic surface, and energy released by gas phase chemical reactions. Solid phase conservation of energy relates axial heat conduction in the substrate, radial convection of

heat to the gas phase, and heat released by chemical reaction on the surface. Momentum conservation balances the axial momentum flux with pressure drop and wall friction effects. The final conservation equation provides for the continuity of mass flow through the system. An equation of state for the gas phase and a reaction stoichiometry for oxygen-fuel reaction complete the equation set. Specification of the reaction equations (heterogeneous and homogeneous) along with atom balances provides for analysis of product composition. Table 2.1 presents the above equation set [7].

Solution of the equation set begins by forming dimensionless equations which result in the identification of 13 dimensionless groups characterizing catalytic reactor behavior. The set of differential equations which have to be solved numerically is reduced to four (for a single fuel component) by appropriate algebraic manipulation. These equations relate dimensionless factors for unconverted fuel mass fraction, gas temperature, surface temperature, and gas velocity to dimensionless distance from the catalyst channel entrance. For a fuel mixture, each additional fuel species adds another term to each energy conservation equation and an additional fuel species balance equation. The current version of the computer solution to the catalytic model is written in FORTRAN 77 and utilizes a numerical solution technique available from IMSL. A more detailed description of the model work can be obtained from Yang's thesis [7]. Table 2.2 presents a list of input data required by the computer model.

Table 2.1 Catalytic Reactor Model Conservation Equations[1]

Fuel-species balance (gas-phase)

$$S\frac{d}{dz}(VC_f) + SA_h \exp\left(\frac{-E_{ah}}{RT}\right)(C_f)^{n_f}(C_{o_2})^{n_o} + k\sigma(C_f - C_s) = 0$$

Fuel-species balance (surface)

$$k(C_f - C_s) = A_s \exp\left(\frac{-E_s}{RT_s}\right)C_s$$

Gas-phase energy balance

$$-S_\rho VC_p\frac{dT}{dz} + \sigma h(T_s - T) + S(-\Delta H)A_h \exp\left(-\frac{E_h}{RT}\right)(C_f)^{n_f}(C_{o_2})^{n_o} = 0$$

Solid-phase energy balance

$$S_s\lambda\frac{d^2T_e}{dz^2} - \sigma h(T_s - T) + \sigma(-\Delta H)A_s \exp\left(-\frac{E_s}{RT_s}\right)C_s = 0$$

Momentum equation $$-(\rho V)\frac{dV}{dz} - \frac{dp}{dz} - \frac{\sigma f}{2S}(\rho V)V = 0$$

Continuity equation $$\frac{d}{dz}(\rho V) = 0$$

Equation of state $$p = \frac{\rho}{M}RT = \frac{\rho_0 V_0 R}{M} \bullet \frac{T}{V}$$

Stoichiometry $$\frac{VC_{o_2}}{(VC_{o_2})_o} = 1 - \phi\left(1 - \frac{VC_f}{(VC_f)_o}\right)$$

[1]The symbols used in this table are defined in Yang's thesis[7]

Table 2.2 Catalytic Reactor Model Input Data Required

INDICATE: MONOLITH OR PACKED BED
HYSTERSIS BRANCH (ES)
NUMBER OF BED SEGMENTS
FIT EXPERIMENTAL DATA
PRINT/SAVE/PLOT

PROVIDE THE FOLLOWING INPUT PARAMETERS:

OPERATIONAL:
- gas temperature (K)
- gas pressure (kPa)
- pre-bed velocity (m/s)

SUBSTRATE(S):
- bed length (cm)
- channel diameter (cm)
- open area (%)
- surface/volume (1/m)
- conductivity (W/m/K)

OPERATIONAL/FUEL # 1:
- fuel/air ratio (kg/kg)
- equivalence ratio

CATALYST/FUEL # 1:
- pre-exponential (m/s)
- activation energy (kJ/mol)

FUEL # 1:
- carbon number
- hydrogen number
- chlorine number
- nitrogen number
- molecular weight (kg kmol)
- heat of combustion (kJ/kg)

- std. diffusivity (cm^2/s)
- pre-exponential
- activation energy (kJ/mol)
- fuel reaction order
- oxygen reaction order

REPEAT: For other fuels and subutrate/catalyst segments

CHAPTER THREE
ENTRY LENGTH TRANSPORT EFFECTS

3.1 Dimensionless Groups

An important approach widely applied in almost every branch of engineering is that of dimensional analysis. The results of dimensional analysis identify the following groups as important in heat and mass transport calculations; Nu, Pr, Re, Sh, Sc, Gz.

The primary parameter for heat transfer processes is the heat transfer coefficient h or, alternatively, the heat flux q''_w. The traditional dimensionless form of h is the Nusselt number Nu, which may be identified as the ratio of convection heat transfer to fluid conduction heat transfer under the same conditions, referenced to the channel or tube diameter, that is:

$$Nu = \frac{q''_w(\text{convection})}{q''_w(\text{conduction})} = \frac{hD}{k} \tag{3.1}$$

A Nusselt number of order unity would indicate a convective heat transport little more effective than pure fluid conduction. For laminar flow in a duct, a large Nusselt number means very efficient convection.

Another critical dimensionless parameter composed entirely of fluid properties, called the Prandtl number, is defined as the ratio of momentum diffusivity (υ) to thermal diffusivity (α) of the fluid:

$$Pr = \frac{\upsilon}{\alpha} = \frac{\mu C_p}{k} \tag{3.2}$$

The Prandtl number provides a measure of the relative magnitudes of the momentum and thermal boundary layers. This parameter has a moderate to strong effect on fluid convection, especially for the single-phase cases. It may be loosely interpreted as the ratio of viscous effects to conduction effects and has the following typical range of values:

Fluid	Pr
Liquid metals	0.004-0.003
Gases	0.7-1.0
Water	1.7-13.7
Oils	50-10,000

For high Prandtl number fluids, such as oils, an assumption of a fully established parabolic velocity profile, even though both velocity and temperature are uniform at the tube entrance, does not lead to significant error because the velocity profile is established much more rapidly than the temperature profile. In contrast, for very low Prandtl number fluids, such as the liquid metals, the temperature profile is established much more rapidly than the velocity profile. However, for the Prandtl number range near 1.0, which includes the gas range, the velocity and temperature profiles develop at similar rates along the tube, and the assumption of a fully established velocity profile at the tube entrance can lead to a considerable error in predicted performance. It is this case which is of particular interest for catalytic combustor/incinerator systems.

For a given geometry and temperature difference, the most important parameter that determines the character of a flow is the dimensionless

Reynolds numbers. For flow inside a duct, or internal flow, the ratio of inertia and viscous forces is characterized as follows:

$$Re = \frac{vD}{\upsilon} = \frac{\rho vD}{\mu} \tag{3.3}$$

For flow in tubes and ducts, transition from laminar to turbulent flow is generally assumed to occur at a Reynolds number of 2,300.

In mass transfer problems, Sherwood number, which is analogous to the Nusselt number, is employed to describe the mass transfer coefficient, hm.

$$Sh = \frac{h_m D}{D_{AB}} \tag{3.4}$$

Just as that of Prandtl number correlates convective heat transfer data, so the Schmidt number correlates convective mass transfer data in an analogous manner.

$$Sc = \frac{\upsilon}{D_{AB}} \tag{3.5}$$

The Schmidt number controls the relation between the velocity and concentration distributions. It provides a measure of the relative effectiveness of momentum and mass transport by diffusion in the boundary layers. For gas mixtures the Schmidt number seldom falls

outside the range of 0.5-3.0; in liquids it is always greater than unity and varies over a range of several thousand fold in different systems.

3.2 Heat Transport

Basically convection is the study of conduction in a fluid as enhanced by its "convective transport", that is, its velocity with respect to a solid surface. It thus combines the energy equation, or first law of thermodynamics, with the continuity and momentum relations of fluid mechanics, In forced convection, the fluid has a nonzero streaming motion in the farfield away from the body surface, caused by a pump or fan or other driving force independent of the presence of the body.

Heat (and mass) transfer in catalytic combustion monolith channels can be considered as convective heat (and mass) transport in a tube. Tube cross-section is assumed to be circular, with non-circular sections being approximated by the equivalent hydraulic diameter. Also, assumptions are that all body forces are negligible and that the fluid is forced through the tube by some external means, unrelated to the temperature field in the fluid. Therefore, the fluid is flowing steadily with laminar motion inside a smooth tube. Further, all the laminar-flow solutions considered in this study are based on the approximation of constant fluid properties over the length of the tube.

The following figures show flow entering a uniform straight duct in the entrance region. The no-slip and no-temperature-jump conditions at the tube surface cause velocity and thermal boundary layers to grow, as in Figure 3.1. Since the duct is of finite width, these boundary layers eventually meet in the center. If Pr is not equal to 1, the hydrodynamic and thermal layers grow at significantly different rates. In the entrance region,

the velocity and temperature profiles change in shape, as in Fig. 3.2 and Fig. 3.3. Wall velocity and temperature gradients are high, hence friction and heat transfer are higher than average. After the boundary layers meet, the wall friction and heat transfer coefficient level off and approach constant values in the fully developed region. The distance required to achieve fully developed conditions is called the entrance length, x_e. We distinguish between hydrodynamically fully developed flow (HFD), if Prandtl number is larger than 1; and thermally fully developed flow (TFD), if Prandtl number is less than 1; as illustrated in Figure 3.2 and 3.3. Whereas for Pr=1, the flow have both velocity and temperature profiles developing together and the associated forced convection heat transfer problem is referred to as the combined hydrodynamic and thermal entry length problem, or in short, as the combined entry length problem [6].

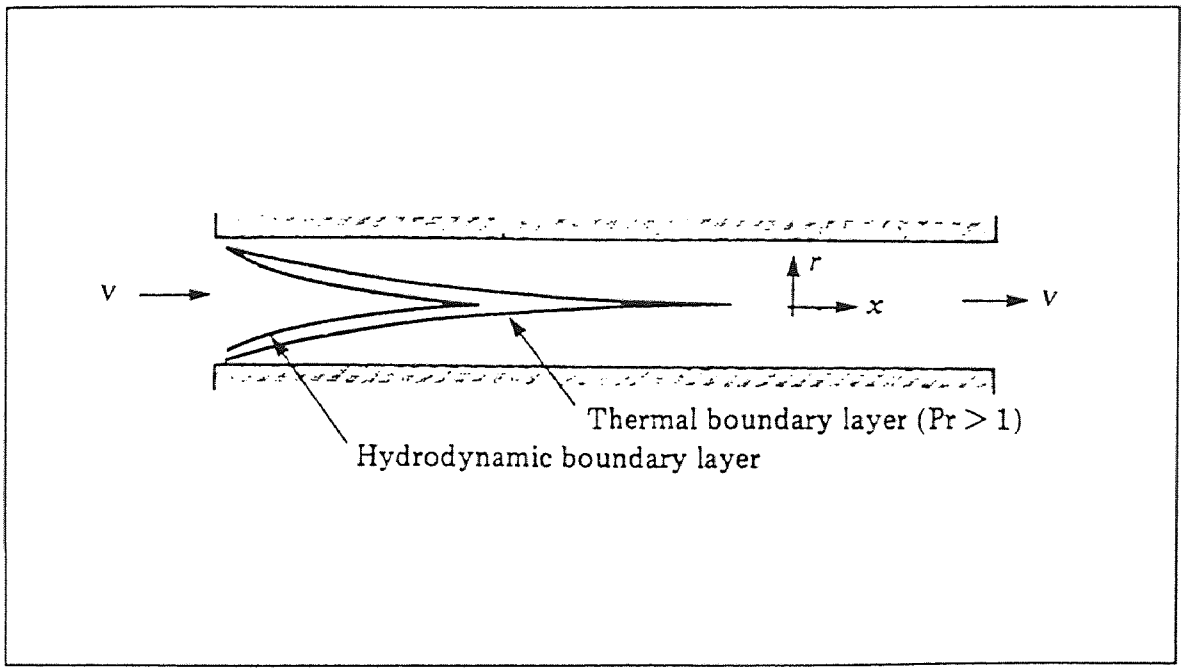

Figure 3.1 Boundary Layer Development

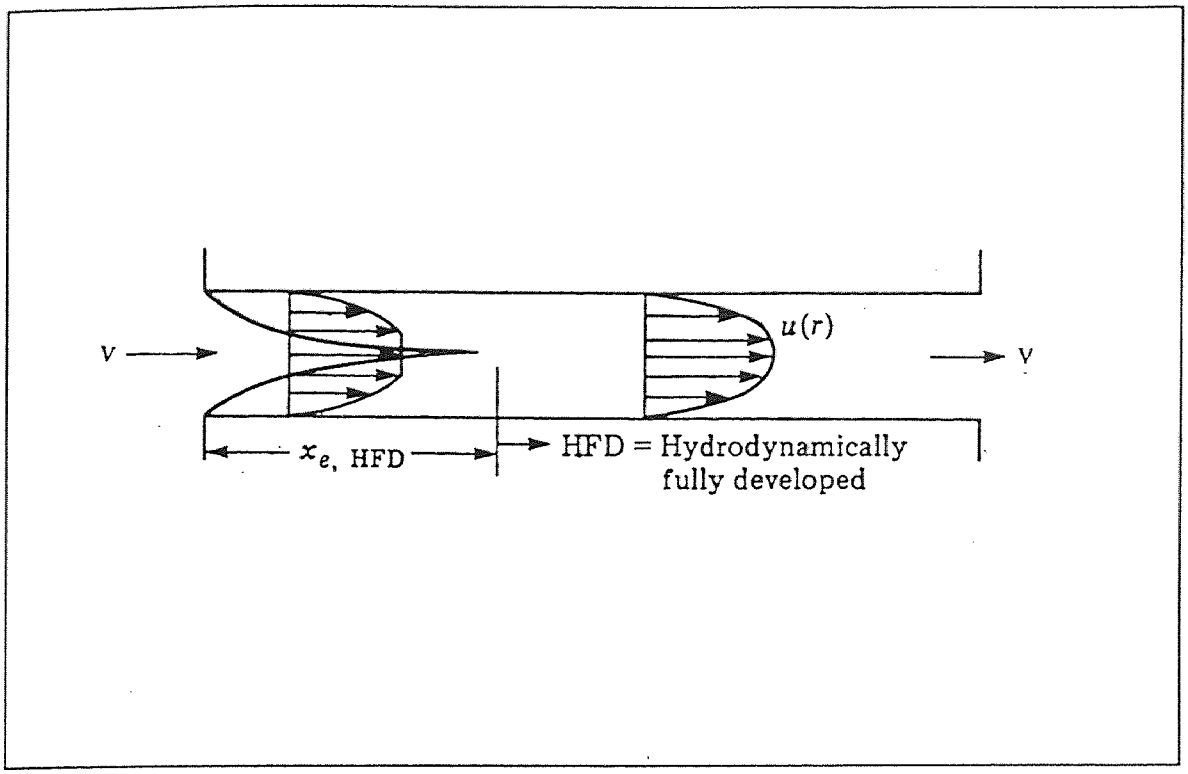

Figure 3.2 Developing Velocity Profiles

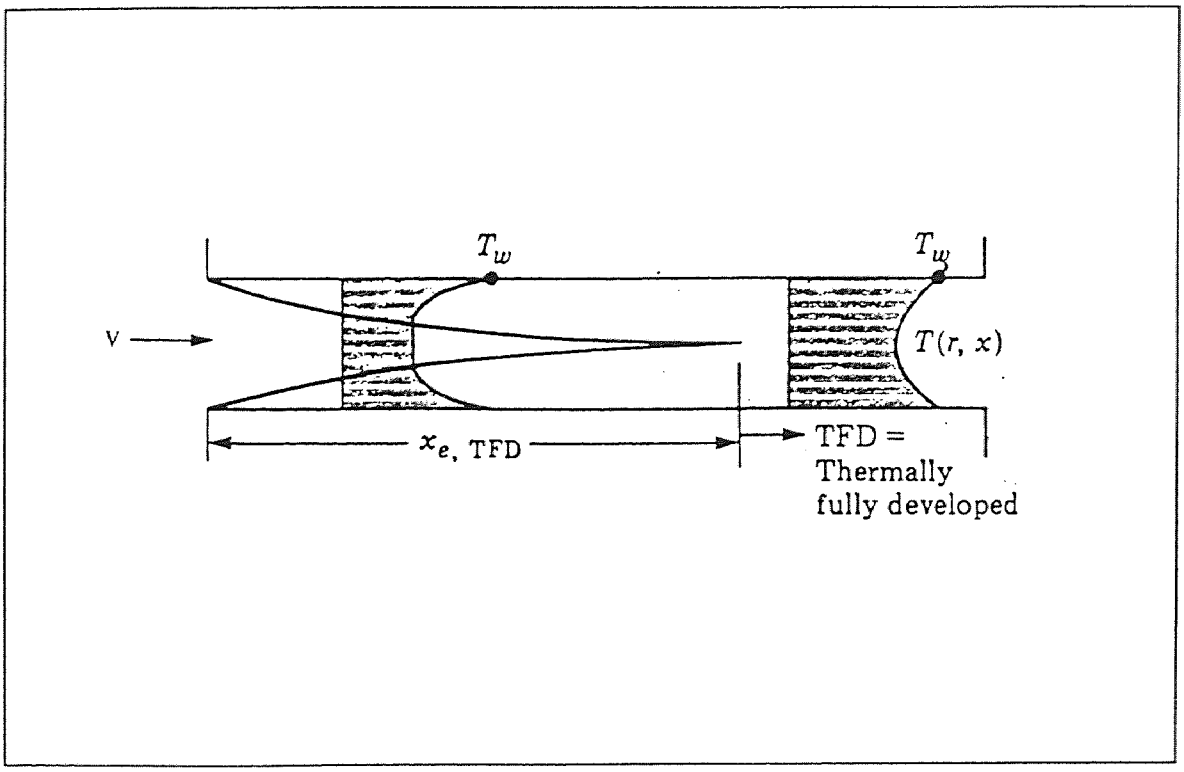

Figure 3.3 Developing Temperature Profiles

If the only heat-transfer mechanism in the tube is by conduction (laminar flow), if properties are constant, and if conversion of mechanical to thermal energy is neglected (low velocity), the following differential equation is obtained for heat transfer [2]:

$$\frac{\partial^2 T}{\partial r^2} + \frac{1}{r} \bullet \frac{\partial T}{\partial r} + \frac{\partial^2 T}{\partial x^2} = \left(\frac{\rho C_p}{k}\right)\left[v \bullet \frac{\partial T}{\partial x} + v_r \bullet \frac{\partial T}{\partial r}\right] \qquad (3.6)$$

For the typical gas-flow problem it may be assumed that conduction in the direction of flow is negligible, and thus the $\partial^2 t/\partial x^2$ term is eliminated. If the velocity distribution is fully established the radial component of the velocity is zero, $v_r=0$, and the term involving v_r is eliminated. However, this work is concerned with the case where the velocity and temperature profiles are not established. In this case, the radial component of the velocity is not zero. An investigation of the relative magnitudes of the various terms of Equation (3.6) reveals that near the tube entrance the term involving v_r is of considerable importance, but that its importance diminishes rapidly away from the entrance. To include the v_r term greatly complicates a numerical solution to Equation (3.6), so for all of the solutions to be considered here the v_r term has been omitted.

In its reduced form, Equation (3.6) can then be a more conveniently expressed by the introduction of the molecular thermal diffusivity of the fluid; α, thus:

$$\frac{1}{r} \bullet \frac{\partial}{\partial r}\left(r\frac{\partial T}{\partial r}\right) + \frac{\partial^2 T}{\partial x^2} = \frac{v}{\alpha}\left(\frac{\partial T}{\partial x}\right) \qquad (3.7)$$

Further, the axial conduction relative to radial conduction be neglected, the energy equation for developing laminar flow in a circular tube can be obtained [3]:

$$\frac{1}{r} \cdot \frac{\partial}{\partial r}\left(r\frac{\partial T}{\partial r}\right) = \frac{v}{\alpha}\frac{\partial T}{\partial x} \tag{3.8}$$

Following the developments presented by Kays [2], Kays et.al. [3], and Shah et.al. [4] a numerical method of solution of entry length region has been previously found. Finite difference was employed to solve the energy equation with the Langhaar velocity profile [8] employed for the axial velocity distribution. For convenient application, Kays used an empirical representation of the Langhaar velocity profiles for constant wall temperature as developed by Hausen [9]. The mean Nusselt number calculation as a function of x/D was presented as follows:

$$Num = 3.66 + \frac{0.104Gz}{1 + 0.016\,(Gz)^{0.8}} \tag{3.9}$$

Where:

$$Gz = \frac{RePr}{x/D} \tag{3.10}$$

In order to more explicitly describe the heat transfer coefficient variation with the entrance length, a local Nusselt number should be used.

Since the mean of the local Nusselt numbers, Num, averaged with respect to the tube length; is expressed as:

$$Num = \frac{1}{x}\int_0^x Nux\,dx \tag{3.11}$$

the local Nusselt number is then given as:

$$Nux = \frac{d}{dx}[xNum] \tag{3.12}$$

From Equation (3.9) and (3.12), we derive the empirical representation of constant wall temperature, Langhaar velocity profiles, local Nusselt number in a circular tube:

$$Nux = 3.66 + \frac{0.00133\,(Gz)^{1.8}}{[1 + 0.016\,(Gz)^{0.8}]^2} \tag{3.13}$$

A comparison, between the equation for local Nusselt number (3.13) derived from Kays mean Nusselt number and Kays numerical data for local Nusselt number, is shown in Figure 3.4.

3.3 Mass Transport

For mass transfer in the monolith catalysis, the reactants present in the reactant flow must diffuse to the surface of the solid, and reaction products then diffuse back from surface to fluid. The diffusion path may be divided

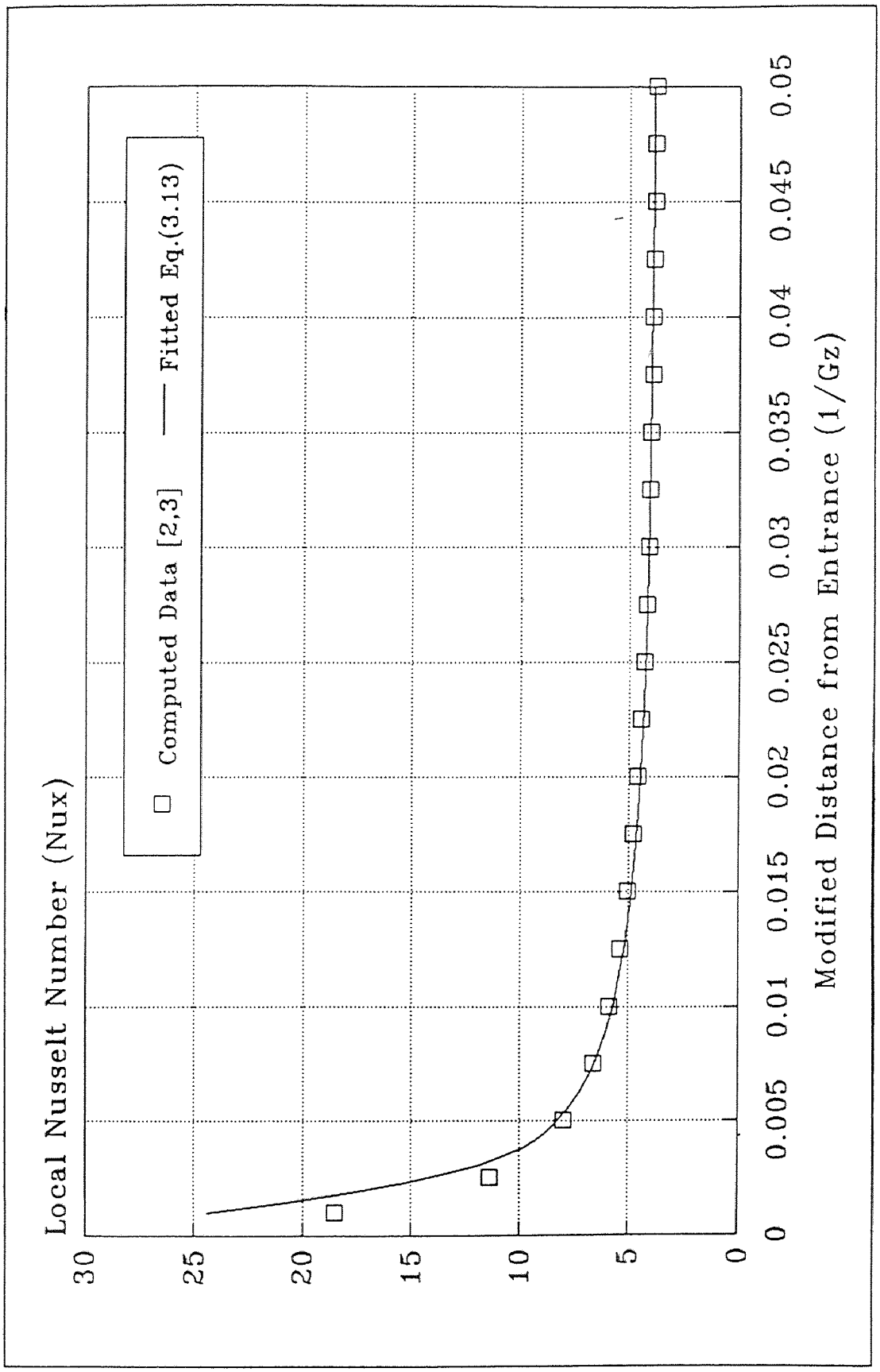

Figure 3.4 Local Nusselt Number in Channel Entry Region (Laminar Flow)

into two parts: bulk fluid to outer surface of the monolith, and from the monolith surface to the active internal surface of the porous solid. For the residence time scales of interest in catalytic combustion, internal diffusion within the pores can be neglected. Fluid passing over the surface of a monolith develops a boundary layer in which the velocity parallel to the surface varies rapidly over a very short distance normal to the flow. The fluid velocity is zero at the substrate surface but approaches the bulk-stream velocity at a plane not far (usually less than a millimeter) from the surface. Mixing occurs in the bulk stream, and reactants and products are transported at rates that depend primarily on the nature of the flow. Very near the surface, the fluid velocity is low and there is little mixing. Transport normal to the surface is by molecular diffusion. In the main fluid stream, mass transfer is essentially independent of the molecular diffusion coefficient D_{AB}, but very near the surface the rate is proportional to D_{AB}. The typical developing mass transfer process is schematically illustrated by the concentration profiles shown in Figure 3.5. Before entering the monolith channel, the concentration shape is uniform and it is gradually changed to a fully developed configuration because of the concentration gradient between wall surface and main stream.

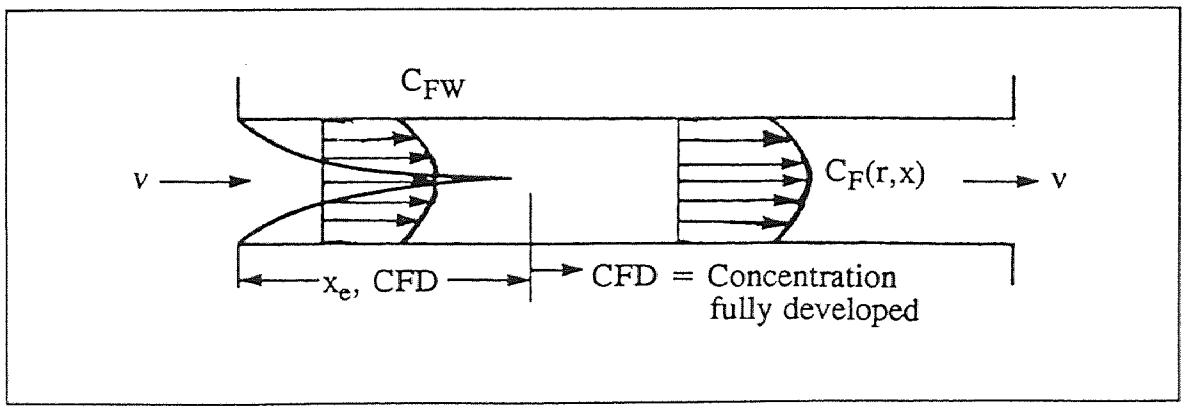

Figure 3.5 Developing Concentration Profiles

According to the transport analogy, if the mass transfer problem has the same geometry, flow pattern, and boundary conditions as the heat transfer problem, then the heat transfer correlations can be converted to mass transfer by using Schmidt number (Sc) and Sherwood number (Sh) to replace Prandtl number (Pr) and Nusselt number (Nu), respectively, in the formulae.

The heat transfer coefficient h is defined by:

$$q''_w = h\,(T_w - T_\infty) \tag{3.14}$$

In an exactly similar manner the mass transfer coefficient hm is defined in either mass or molar diffusion form:

$$G_{Aw} = h_m\,(\rho_{Aw} - \rho_{A\infty}) \tag{3.15}$$

or

$$G_{Aw} = h_m\,(C_w - C_\infty) \tag{3.16}$$

By analogy with heat transfer mass transport correlates with flow parameters in the following dimensionless form:

$$Sh = 3.66 + \frac{0.00133\,(Gzm)^{1.8}}{[1 + 0.016\,(Gzm)^{0.8}]^{2}} \qquad (3.17)$$

where:

$$Gzm = \frac{ReSc}{x/D} \qquad (3.18)$$

CHAPTER FOUR

INFLUENCE OF ENTRY BOUNDARY LAYER DEVELOPMENT ON FUEL CONVERSION

The expression for entry length local Nusselt number (equation 3.13) and local Sherwood number (equation 3.17), provide the necessary transport relations to account for entry effects in catalytic combustion systems. These equations were inserted into the modeling program in subroutines FCNEQN and FCNJAC (see Appendix: Program Source File). FCNEQN represents the double boundary value equation set which must be solved and FCHJAC presents the Jacobian which is required in the solution approach. Both transport equations indicate rates which become infinitely large as distance from the entrance approaches zero. To avoid possible problems in obtaining a numerical solution, the heat transport rate (and by analogy the mass transport rate) was "capped" so as not to exceed Nusselt number values of approximately 500. The rapid change in transport properties with initial distance from the entrance was accommodated by an automatic step change initiated by the program in this region. A complete program listing is provided in Yang's thesis [7].

As discussed in the previous sections, the entry length effects considered account for simultaneous development of the velocity, temperature, and concentration profiles. The influences of these effects on catalytic combustor performance are to be compared with the previous approach which assumed constant transport rates over the entire length of the catalytic bed. For this purpose, characteristic combustor operating conditions were used, as presented in Table 4.1, to evaluate performance with and without entry length considerations. A stoichiometric methane-air

Table 4.1 Typical Model Input Parameters

No.	Item	Value	Unit
1.	Initial gas temperature	500-900	K
2.	Initial gas velocity	15.1	m/s
3.	Initial pressure	101.3	kPa
4.	Fuel-air ratio (weight)	0.0142	kg/kg
5.	Equivalence ratio	0.2451	kg/kg
6.	Molecular weight of fuel	16.0	kg/kmol
7.	Carbon number of fuel	1.0	
8.	Hydrogen number of fuel	4.0	
9.	Reactant diffusivity (at T=273 K)	0.1826	m^2/s
10.	Catalyst activation energy	60.0	kJ/mol
11.	Catalyst pre-exponential factor	500.0	m/s
12.	Homogeneous activation energy	121.34	kJ/mol
13.	Homogeneous pre-exponetial factor	9,800.0	
14.	Homogeneous reaction order for fuel	1.0	
15.	Homogeneous reaction order for oxygen	1.0	
16.	Heat of combustion	50,000.0	kJ/kg
17.	Substrate conductivity	3.5	J/m.s.K
18.	Catalyst channel length	3.8-11.4	cm
19.	Catalyst channel diameter	0.114	cm
20.	Open area fraction	0.549	
21.	Ratio of surface area to volume	4,271.0	1/m
22.	Chlorine number of fuel	0.0	
23.	Nitrogen number of fuel	0.0	

mixture was assumed with both gas phase and surface reaction allowed. Inlet reactant temperature was varied from 500 ^{o}K to 900 ^{o}K. Substrate properties and catalytic reaction rates used are typical of platinum on corderite, with bed length varying from 3.8 cm to 11.4 cm.

4.1 Fuel Conversion Versus Bed Length

Figures 4.1 to 4.8 present fuel conversion as a function of distance from the bed entrance divided by bed length (L/D) for L/D=33 and L/D=100, respectively. For each figure, reactant inlet temperatures of 600 ^{o}K, 700 ^{o}K, 800 ^{o}K and 900 ^{o}K are considered, and the influences of neglecting entrance effects and not neglecting entrance effects are displayed.

As expected, increasing inlet gas temperature results in increasing fuel conversion in all cases. No evidence is exhibited of initiation of gas phase reactions and thus fuel conversion is controlled by diffusion and/or surface reaction in all cases. Detailed analysis of curves for L/D=33 and L/D=100 indicates that curves for the former condition are simply a sub-set of those for the larger L/D ratio, and thus represent comparable behavior. It is expected that increased substrate conductivity could result in different L/D ratios giving distinct solutions. Additional investigation of the effect on catalytic performance of increased substrate conductivity needs to be performed for applications where metallic substrates are to be employed.

The most interesting and unexpected feature of these curves is the change in which assumption, constant transport rates (no entrance effect) or entry varying transport rates (entrance effect), results in higher fuel conversion as the inlet reactant temperature is increased. The serious limitation of assuming constant transport is discussed in the next section.

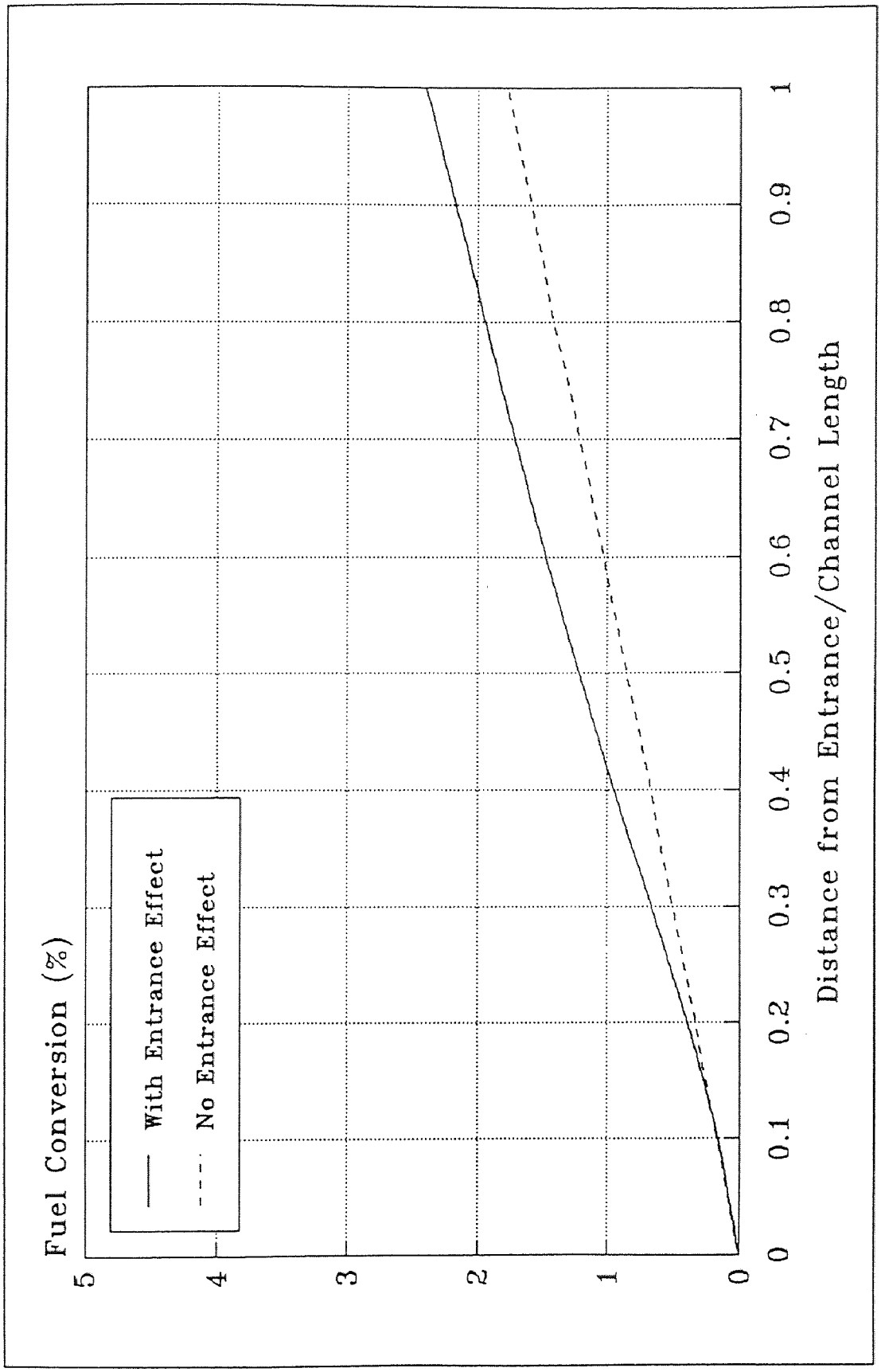

Figure 4.1 Entrance Length Effect Catalytic Monolith (T=600 K, L/D=33)

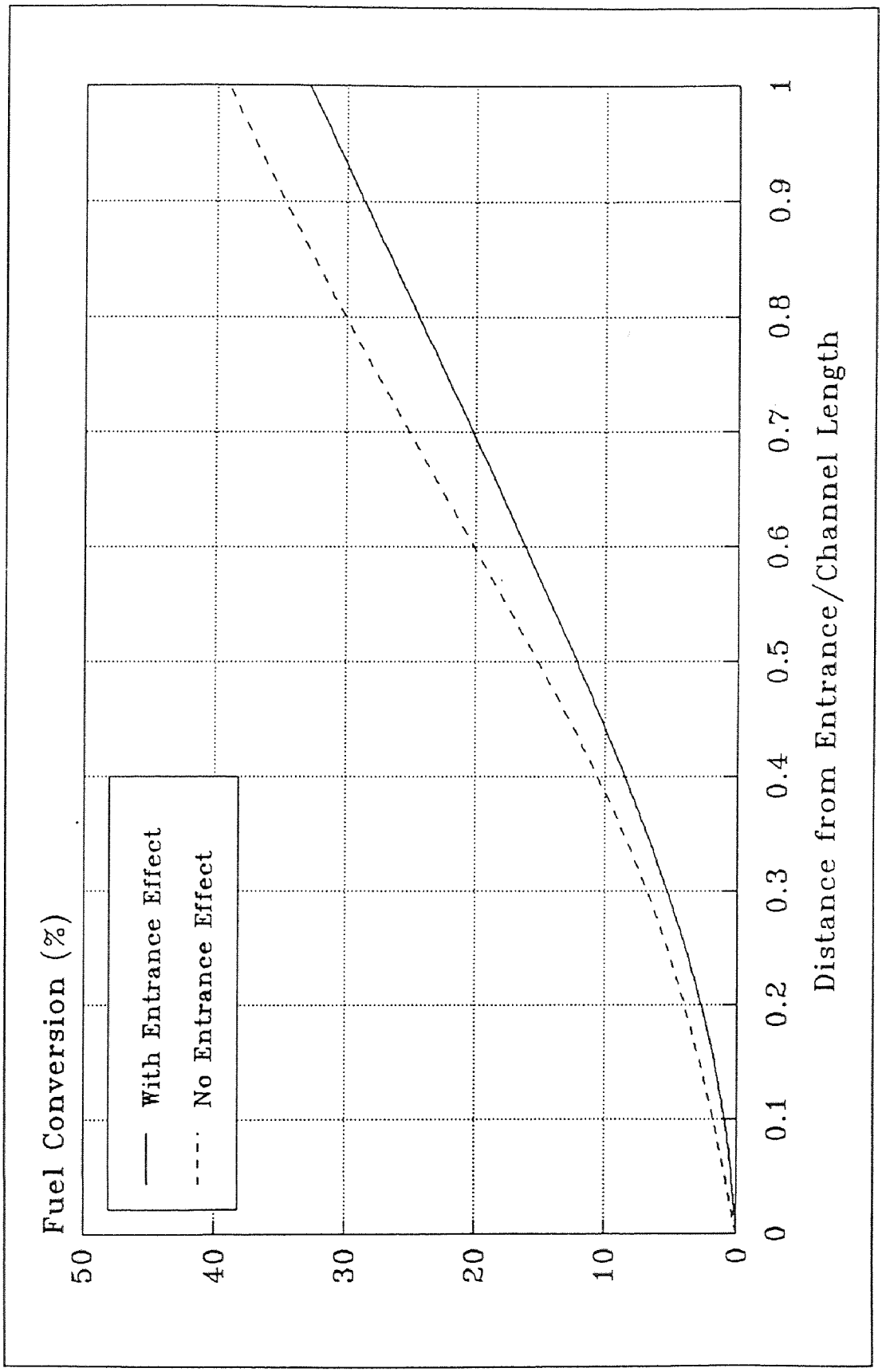

Figure 4.2 Entrance Length Effect Catalytic Monolith (T = 700 K, L/D = 33)

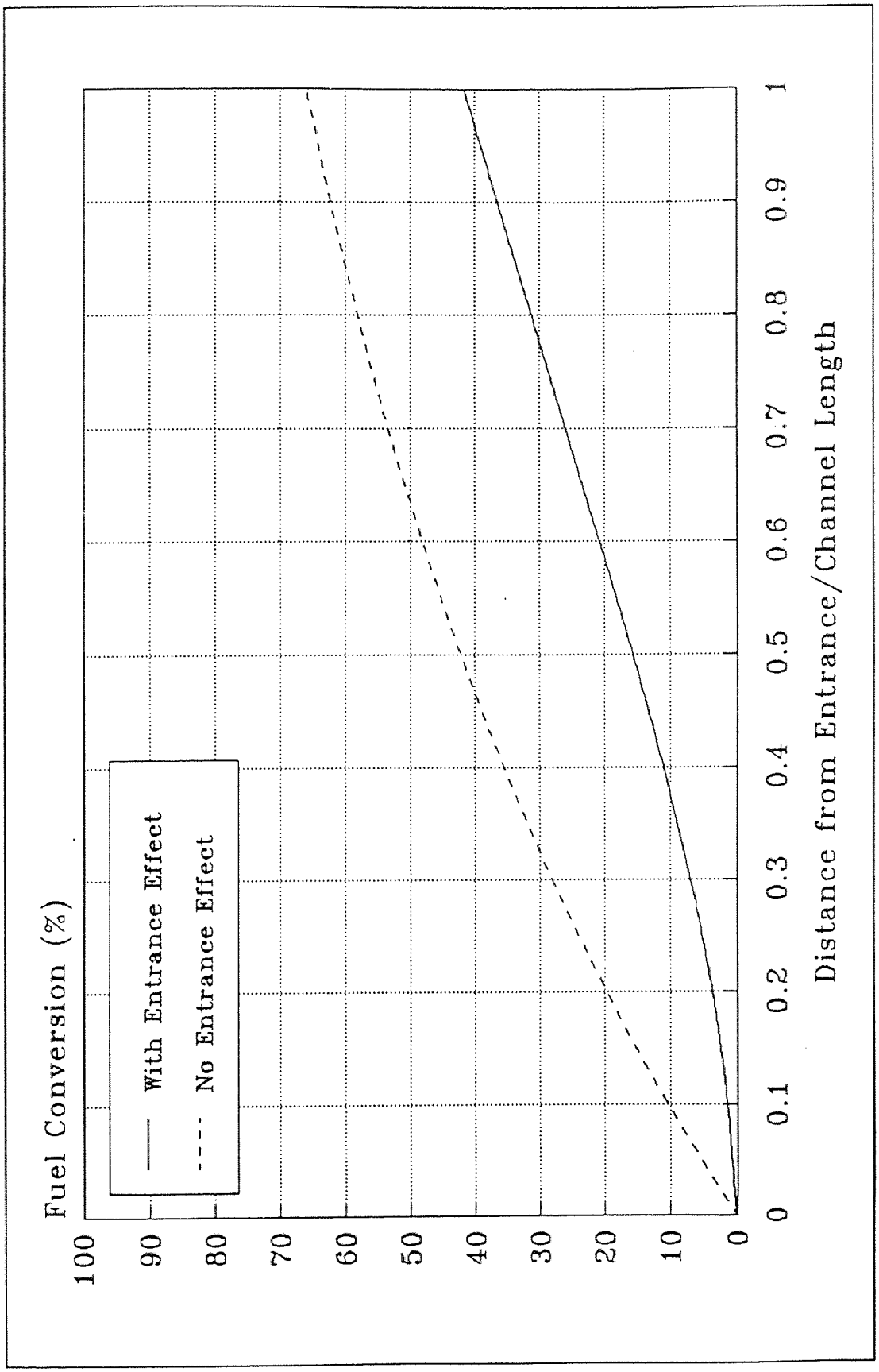

Figure 4.3 Entrance Length Effect Catalytic Monolith (T = 800 K, L/D = 33)

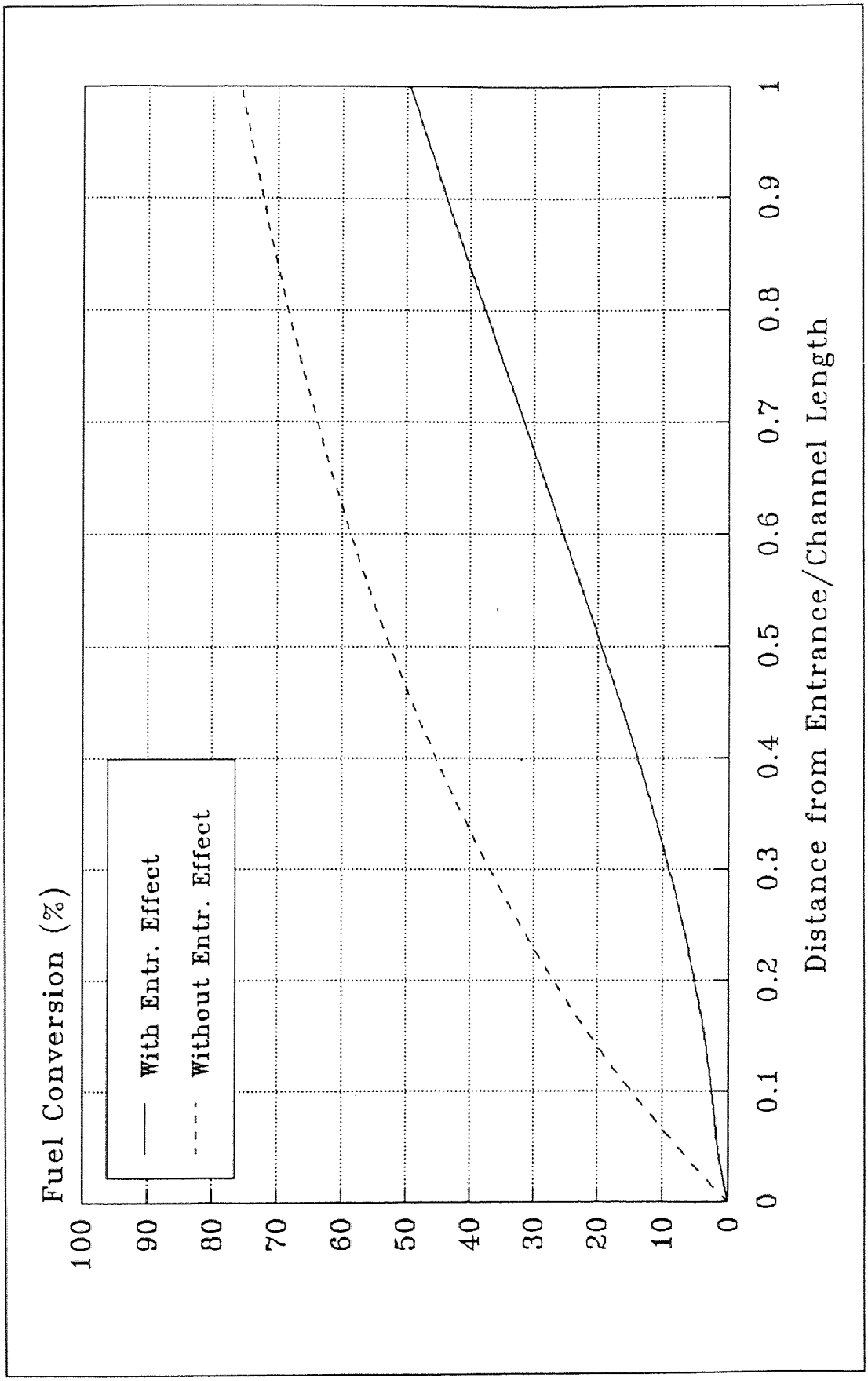

Figure 4.4 Entrance Length Effect Catalytic Monolith (T = 900 K, L/D = 33)

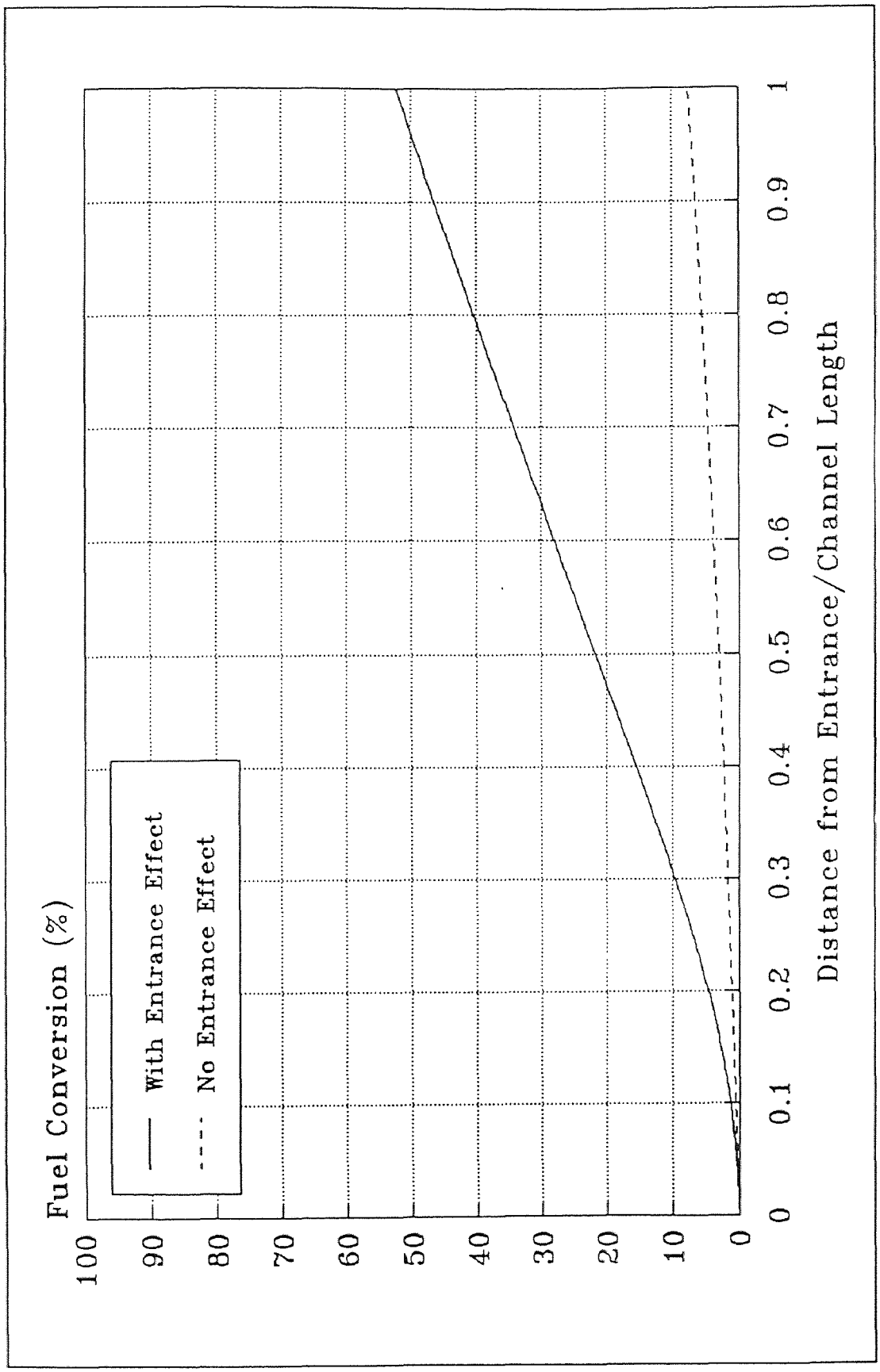

Figure 4.5 Entrance Length Effect Catalytic Monolith (T=600 K, L/D=100)

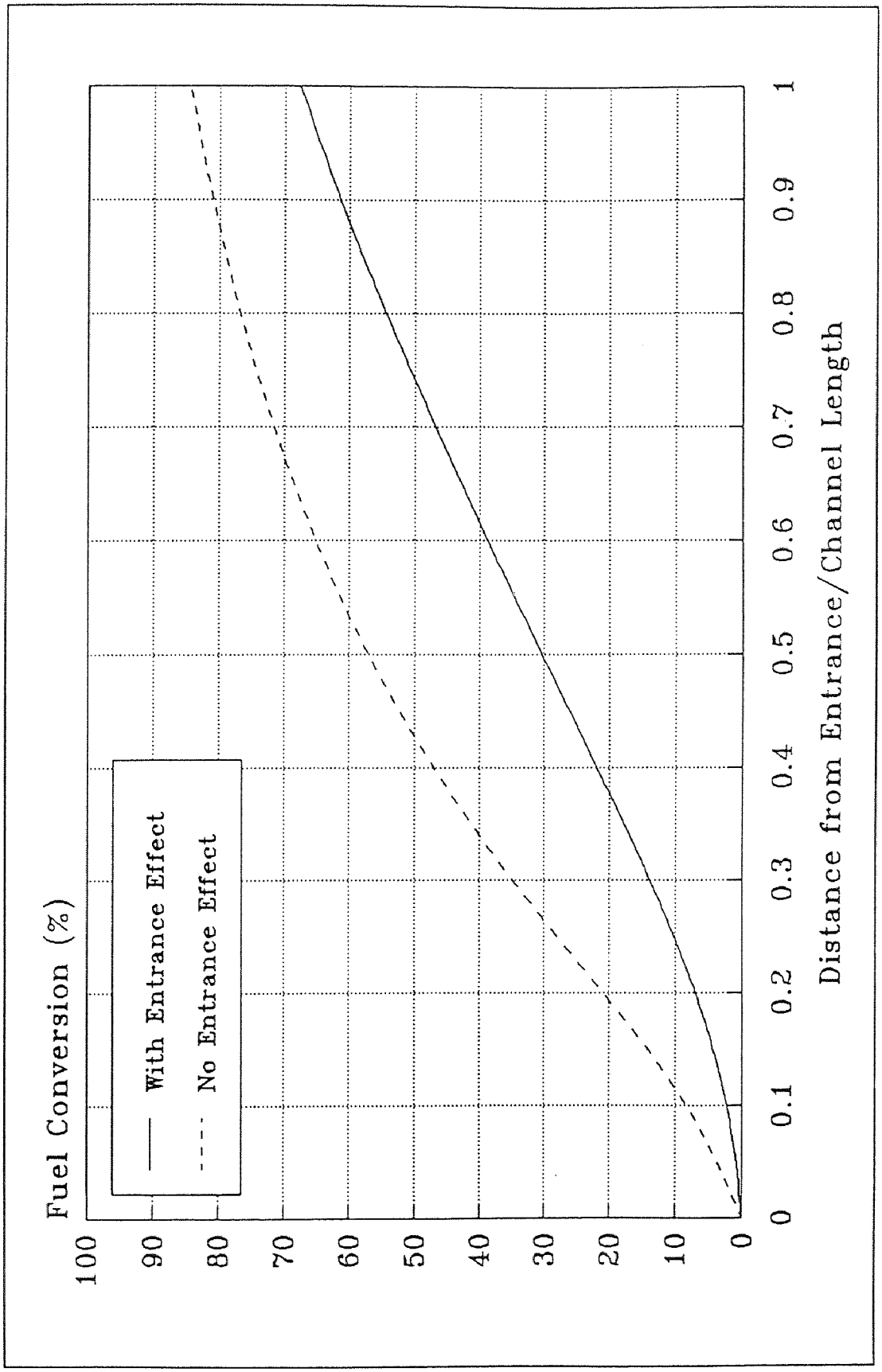

Figure 4.6 Entrance Length Effect Catalytic Monolith (T = 700 K, L/D = 100)

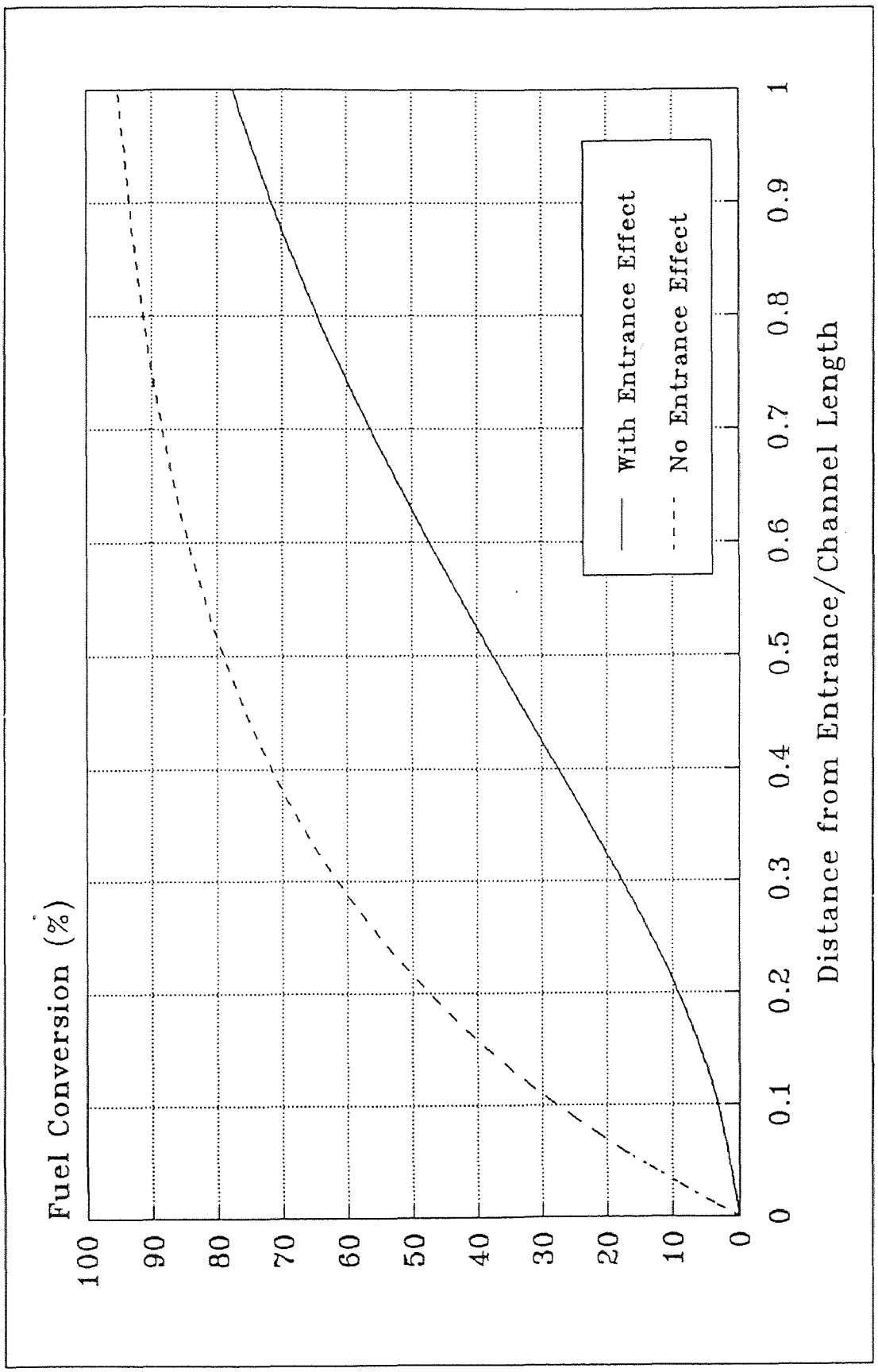

Figure 4.7 Entrance Length Effect Catalytic Monolith (T = 800 K, L/D = 100)

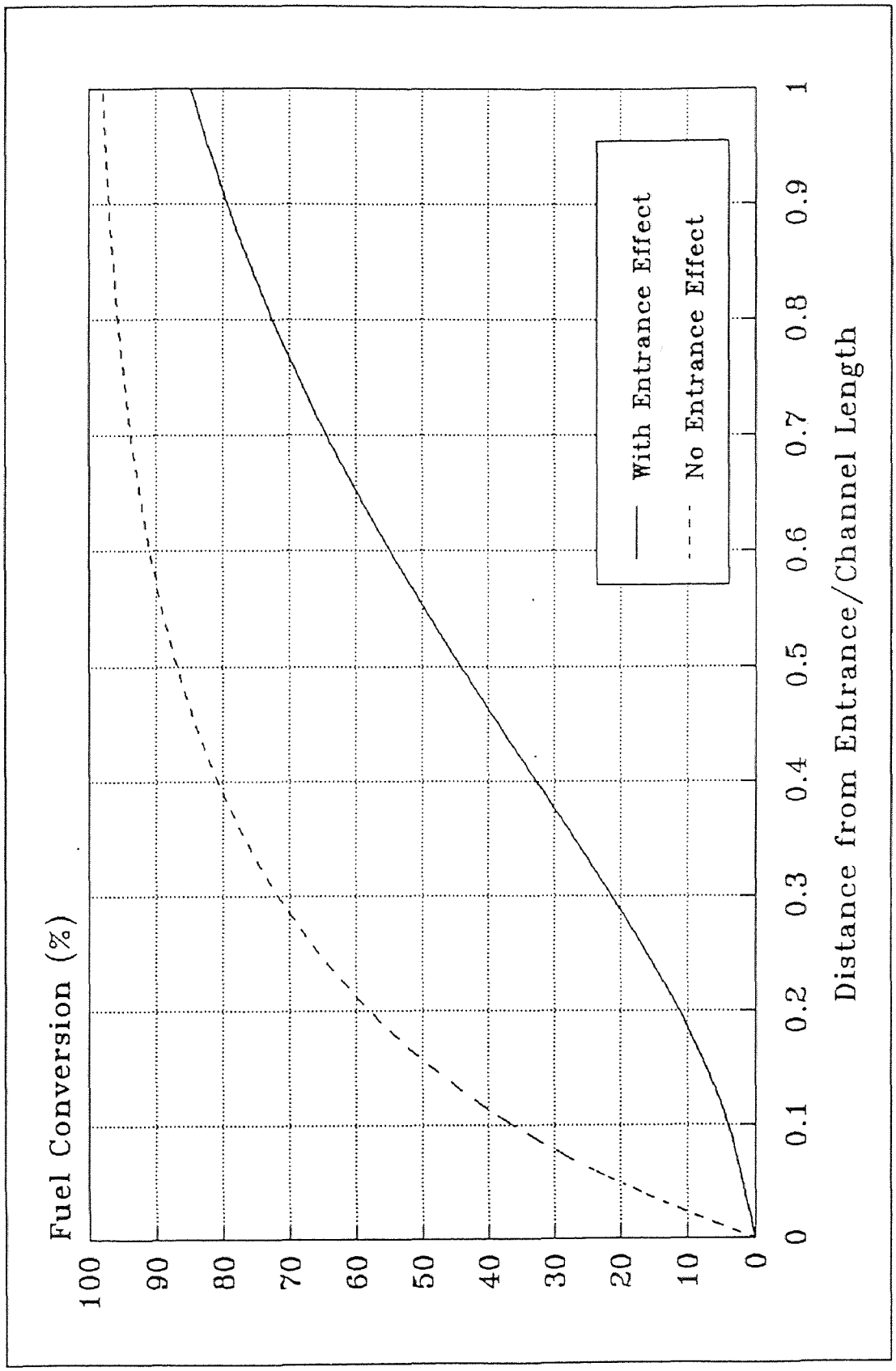

Figure 4.8 Entrance Length Effect Catalytic Monolith (T = 900 K, L/D = 100)

4.2 Conversion Versus Reactant Inlet Temperature

The effect of entry length on overall fuel conversion (bed exit fuel conversion) as a function of reactant inlet temperature is illustrated in Figure 4.9 for L/D=33 and Figure 4.10 for L/D=100. Both curves show typical catalytic reactor behavior as the inlet temperature is varied. At low temperature (400 ^{o}K to approximately 650 ^{o}K) fuel conversion is controlled by surface reaction rate. Increasing temperature results in higher surface temperature, and due to the Arrhenious behavior, an exponentially increasing reaction rate (conversion). The leveling-off of the conversion rate in the high temperature region (650 ^{o}K to 900 ^{o}K) results from diffusional transport to the surface becoming a limiting step in the fuel conversion process. If gas phase reaction occurs, we expect a second occurrence of rapidly increasing fuel conversion as temperature is increased further. Since this is not exhibited in the cases presented, it can be assumed that no substantial gas phase reaction is occurring.

As indicated previously, the most interesting phenomena evidenced in the fuel conversion vs. reactant inlet temperature curves is the crossing of the curves representing the inclusion of entrance length effects (solid curve) and no entrance length effects (dashed curve). In the low temperature region, the presence of a thinner initial boundary layer results in increased conversion and a more rapidly rising fuel conversion curve. In catalytic technology this is referred to as an improvement in catalytic light-off. However, in the high temperature region the thinner initial boundary layer results in decreased overall fuel conversion. Consequently, increased catalyst bed length will be needed to achieve efficient fuel conversion. Recognition of these differing effects will be especially important in catalytic combustion systems which employ segmented bed operation. In

these systems, the re-starting of the boundary layer flow at the entrance of each bed will have a substantial influence on overall fuel conversion.

The behavior exhibited in Figures 4.9 and 4.10 can be best explained by considering the surface reaction rate equation. An Arrhenious expression for surface reaction rate can be written as follows:

$$RR_{surface} = (C_{surface\ fuel})[Exp\ (-E_{cat}/RT_{surface})] \qquad (4.1)$$

In this equation the surface reaction rate is taken as first order in surface fuel concentration and zero order in surface oxygen concentration, as has generally been found applicable in catalytic combustion reactors. Surface temperature ($T_{surface}$) appears as a negative reciprocal in the exponential term in which the activation energy for the surface reactions (E_{cat}) is assumed constant. This equation must be connected with the influence of the thinner boundary layer present over the tube entry length. This thinner layer results in higher transport of both heat and mass. As a result, reduced surface temperature and increased surface fuel concentrations occur.

At low temperature, the increase in heat loss is not substantial since the temperature difference between the surface and the gas phase is small. Thus only minor reductions in surface temperature are expected. However, substantial differences in mass transport of fuel to the surface occurs due to the higher Sherwood numbers in comparison with no entry length assumptions. Consequently, the surface fuel reaction rate increases since the surface fuel concentration increases.

At high temperature, substantial heat loss occurs due to the increased surface temperature (resulting from increased fuel conversion) in combination with the reduced boundary layer thickness for entry length

conditions. A reduced surface temperature is also experienced beyond the entry region due to substrate conduction. Since surface reaction rate is exponentially dependent on surface temperature, the result is a substantial reduction in overall fuel conversion. For example, using the shorter bed segment (L/D=33) at 900 ^{o}K inlet reactant temperature, the overall fuel conversion is reduced to 50% when entry effects are considered compared with an overall fuel conversion of 75% if constant transport properties are assumed.

Figures 4.11 and 4.12 illustrate the variation of surface temperature and surface fuel concentration with distance from the monolith entry for an inlet temperature of 700 ^{o}K and L/D ratio of 100. It should be noted that as used here, surface concentration refers to the fuel gas phase concentration immediately adjacent to the surface. True surface concentration (e.g. moles/sq. meter) would require detailed specification of adsorption/desorption behavior. Since these details are not part of the model, the adjacent gas phase concentrations are used as surrogates to represent the actual surface concentration.

The initial section of both curves near the channel entrance exhibit the influence of the reduced boundary layer thickness on increasing transport rates. In this region the entrance effects result in decreased surface temperature and increased surface concentration. Since the reactant inlet temperature chosen for these curves (T=700 ^{o}K) was in the upper temperature region, subsequent behavior is dominated by the influence of temperature. While the curves with and without entrance effects differ in the remained of the channel the magnitudes of surface temperature and fuel concentration are comparable. Consequently, the initially reduced fuel conversion due to entrance effect is never overcome and a reduced fuel

conversion is experienced over the entire monolith channel length. A graph of gas phase fuel concentration as a function of distance from the entrance presents a complimentary representation of fuel conversion as shown in Figure 4.13 for the same conditions as given in Figure 4.11 and 4.12. Persistence of the higher fuel concentrations throughout the monolith channel as a result of the entrance effect is remarkable. The presence of entry effects increases the required monolith length by some 30 to 40% for the same overall fuel conversion to be achieved.

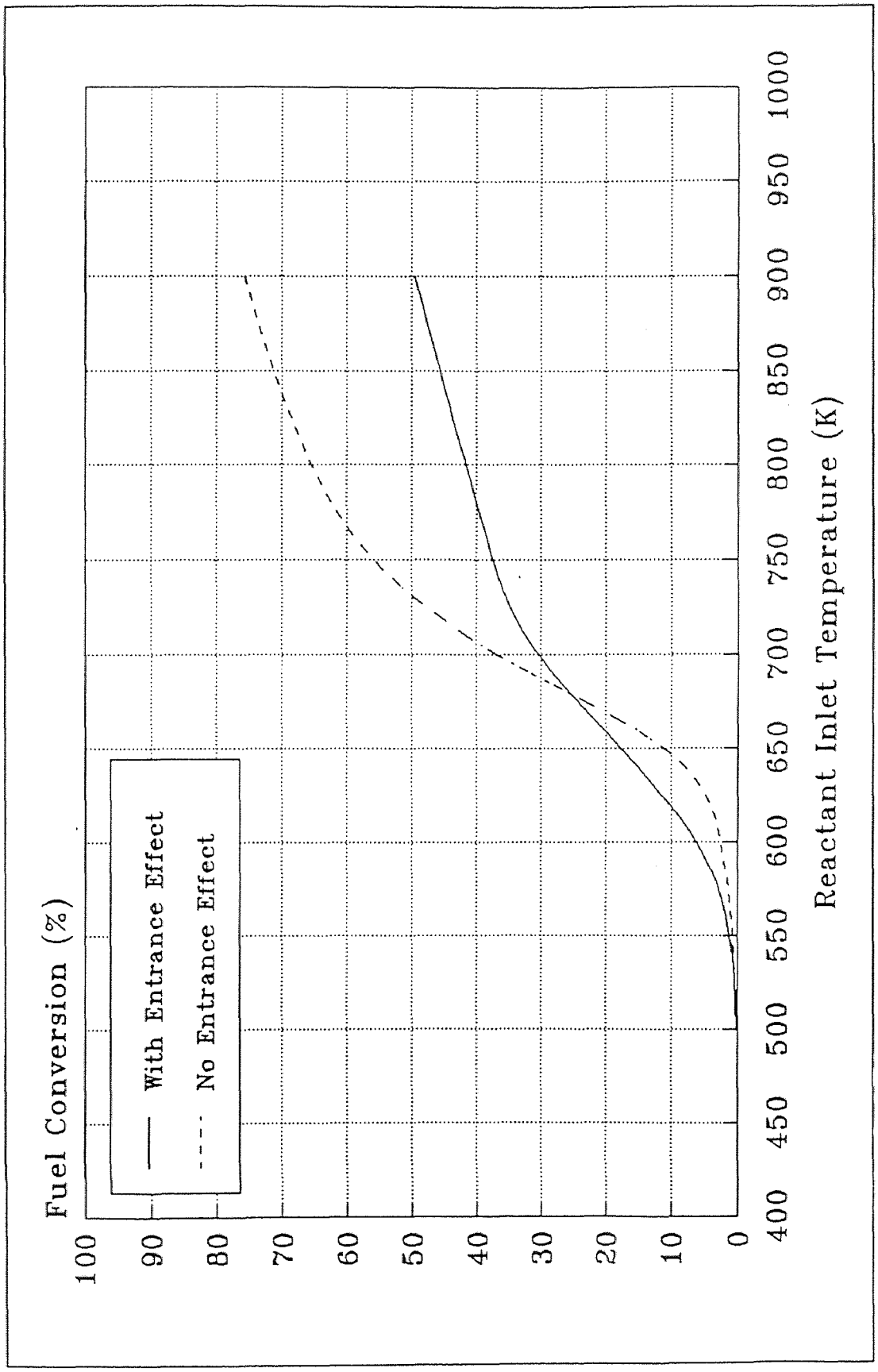

Figure 4.9 Entry Effect on Conversion of Fuel vs. Inlet Temperature (L/D=33)

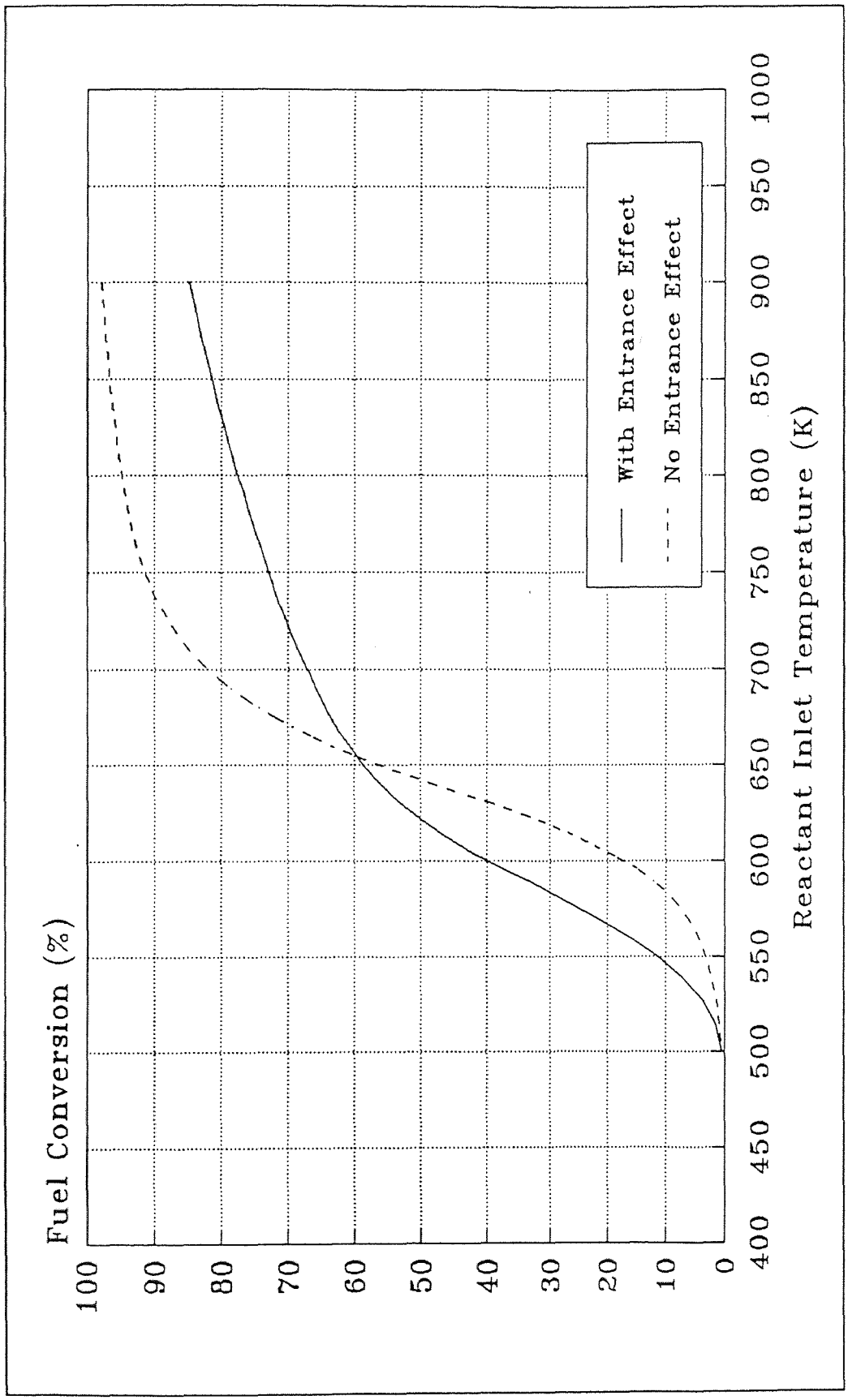

Figure 4.10 Entry Effect on Conversion of Fuel vs. Inlet Temperature (L/D=100)

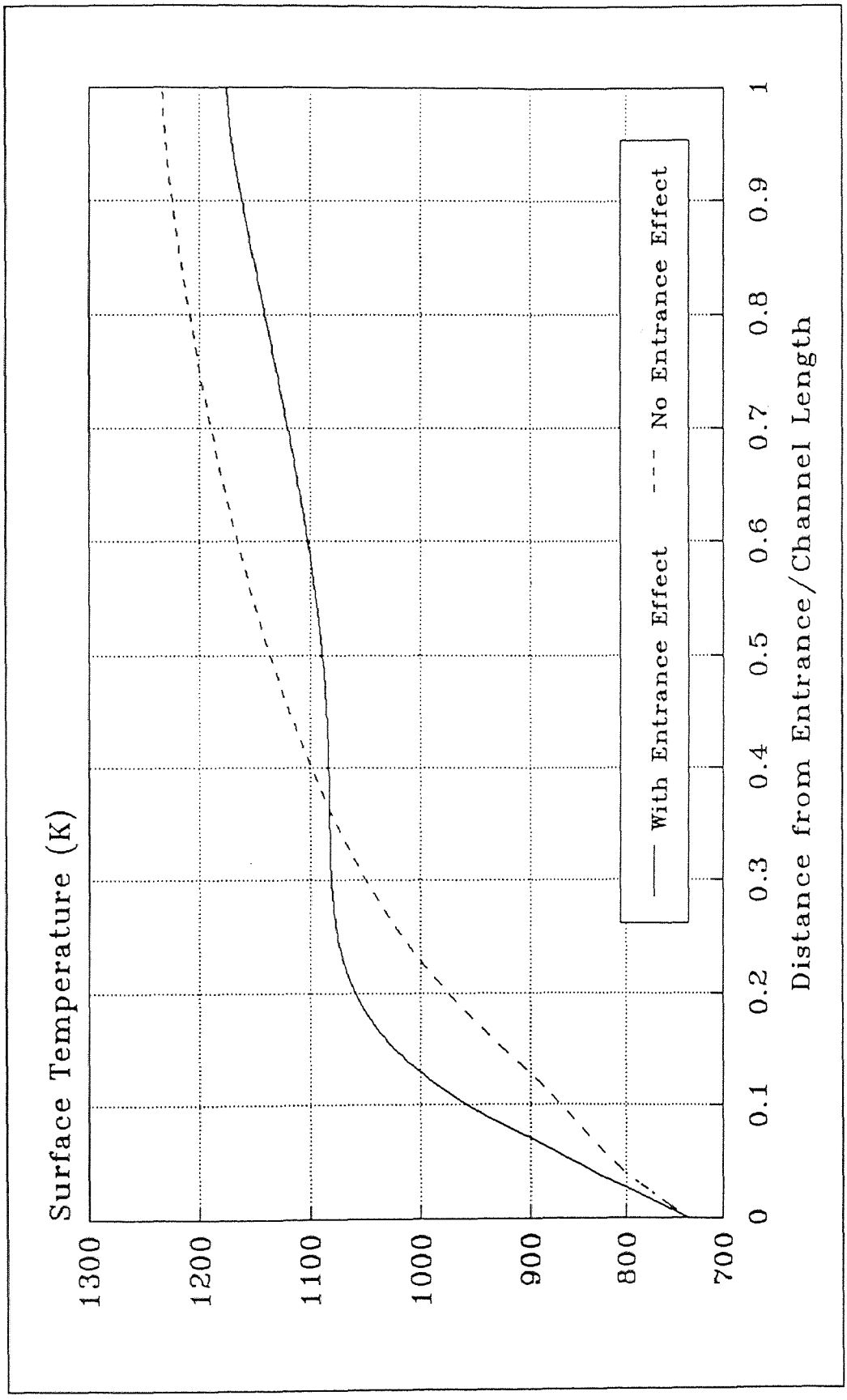

Figure 4.11 Entry Length Effect, Surface Temperature (T = 700 K, L/D = 100)

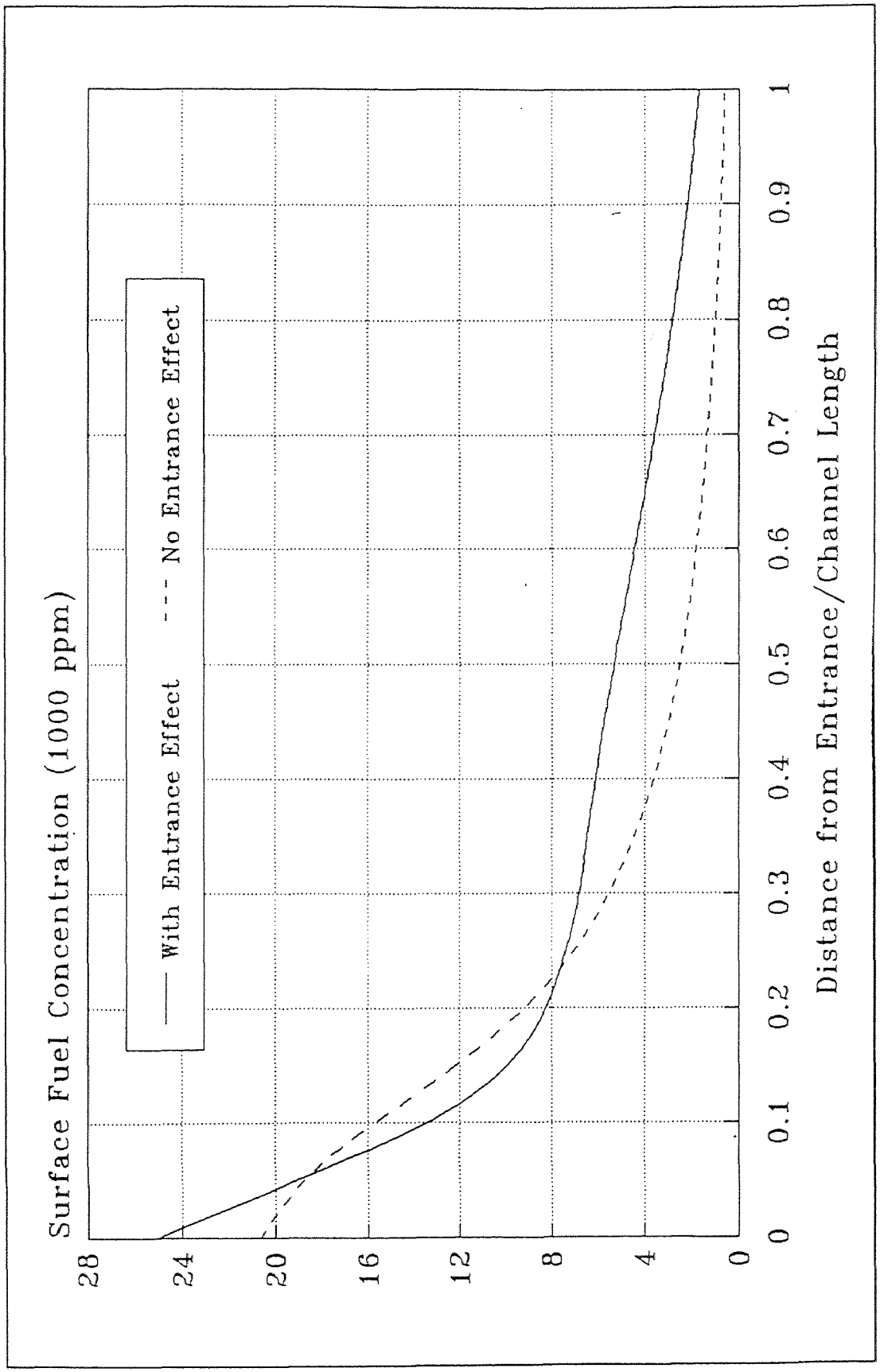

Figure 4.12 Entry Length Effect, Fuel Surface Concentration (T=700 K, L/D=100)

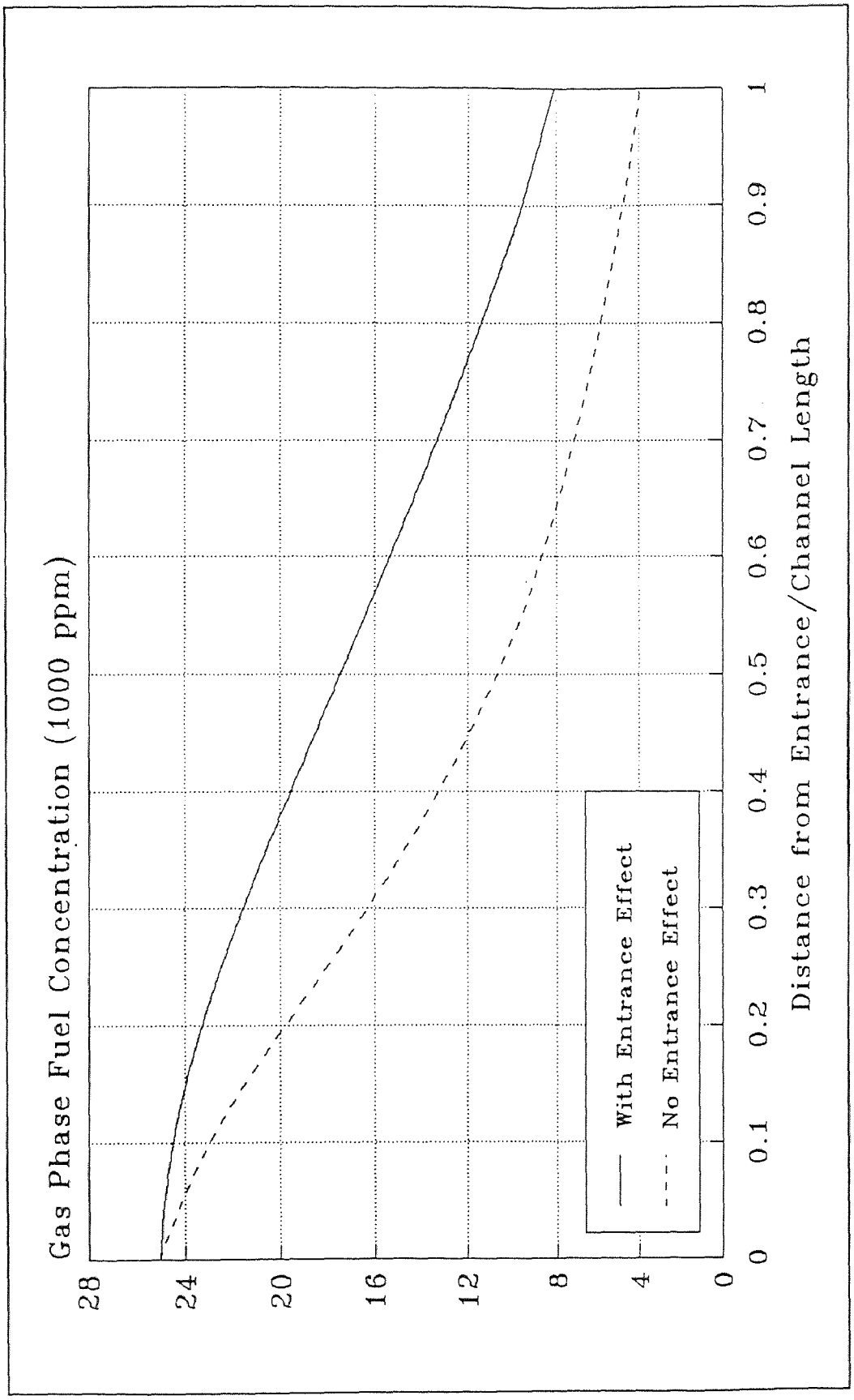

Figure 4.13 Entry Length Effect, Fuel Gas Concentration (T = 700 K, L/D = 100)

CHAPTER FIVE
COMMENTS ON TURBULENT FLOW CONDITIONS

It has been found by experiment that laminar flow occurs for flow inside round smooth tubes for Reynolds numbers less than about 2,300. Using the concept of equivalent diameter (hydraulic diameter), this result is also applied to other cross-sectional shapes. Above this Reynolds number the flow becomes unstable to small disturbances, and a transition to a turbulent type of flow generally occurs, although a fully established turbulent flow may not occur until the Reynolds number reaches about 10,000.

The turbulent tube-flow problem is further complicated by the fact that the turbulent boundary-layer development is very strongly influenced by the character of the typical tube entrance. If a boundary-layer trip is provided, then the combined hydrodynamic and thermal-entry-length behavior is close to that predicted for fully turbulent flow. However these are laboratory conditions that are seldom encountered in real applications. If the boundary layer is not tripped, a laminar boundary layer tends to develop, and, depending on the Reynolds number and the free-stream turbulence, it is possible to get fully developed laminar flow before a transition to turbulent flow occurs. In the typical monolith catalytic bed segment, a sharp-edged contraction is experienced by the flow. Consequently, there is a separated flow at the entrance with sufficient vorticity shed into the main stream that the heat-transfer and mass transfer rates are very much higher than would be obtained in a smoothly developing boundary layer [2].

At present we must rely on experimental data for the turbulent-flow entry region of a pipe for most applications. From Kays development [3],

Figures 5.1, 5.2, and 5.3 show the thermal-entry-length effect for turbulent flow in a circular tube for constant heat rate for a number of different cases. At Pr=0.01 the effect is rather pronounced and increases with Reynolds number (Fig. 5.1). Figure 5.2 illustrates the strong influence of Prandtl number. At Prandtl numbers above 1 the thermal-entry-length effect becomes of decreasing importance. Note in Fig. 5.3 that at Pr=0.7 there is very little influence of Reynolds number. According to this plot character, the following fitted formula to calculate the turbulent flow Nusselt number results:

$$\frac{Nux}{Nu_\infty} = 1.0 + \frac{1.338\left(\frac{D}{x}\right)^{1.3}}{\left[1.0 + 0.0327\left(\frac{D}{x}\right)^{0.1}\right]^{2.5}} \qquad (5.1)$$

Where Nusselt number for fully developed turbulent flow is calculated by using the following equation [10]:

$$Nu_\infty = 0.023\ Re^{0.8}\ Pr^{0.5} \qquad (5.2)$$

Combining Equations (5.1) and (5.2), we finally get an expression of local Nusselt number, Nux, for turbulent flow condition. The comparison of the plot by Kays [3] and the new formula of Nusselt number is presented in Fig. 5.4, and demonstrate excellent agreement. Figure 5.4 also illustrates that in the turbulent flow the influence of entry length effect only exists at very beginning of the tube length. It diminishes rapidly away at distances of x/D larger than 20. Therefore, we can conclude that the entrance length effect on turbulent flow condition will be less important than that of laminar flow.

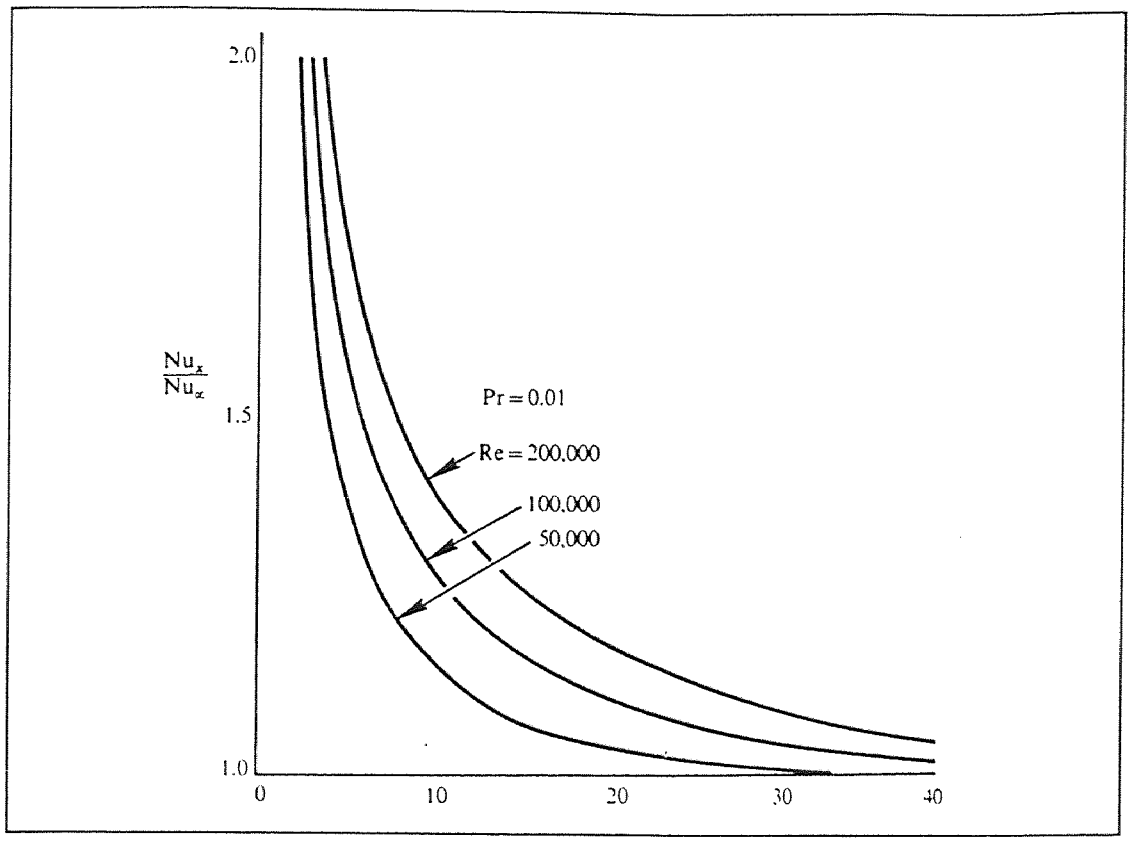

Figure 5.1 Variations of Turbulent Flow with Prandtl Numbers I

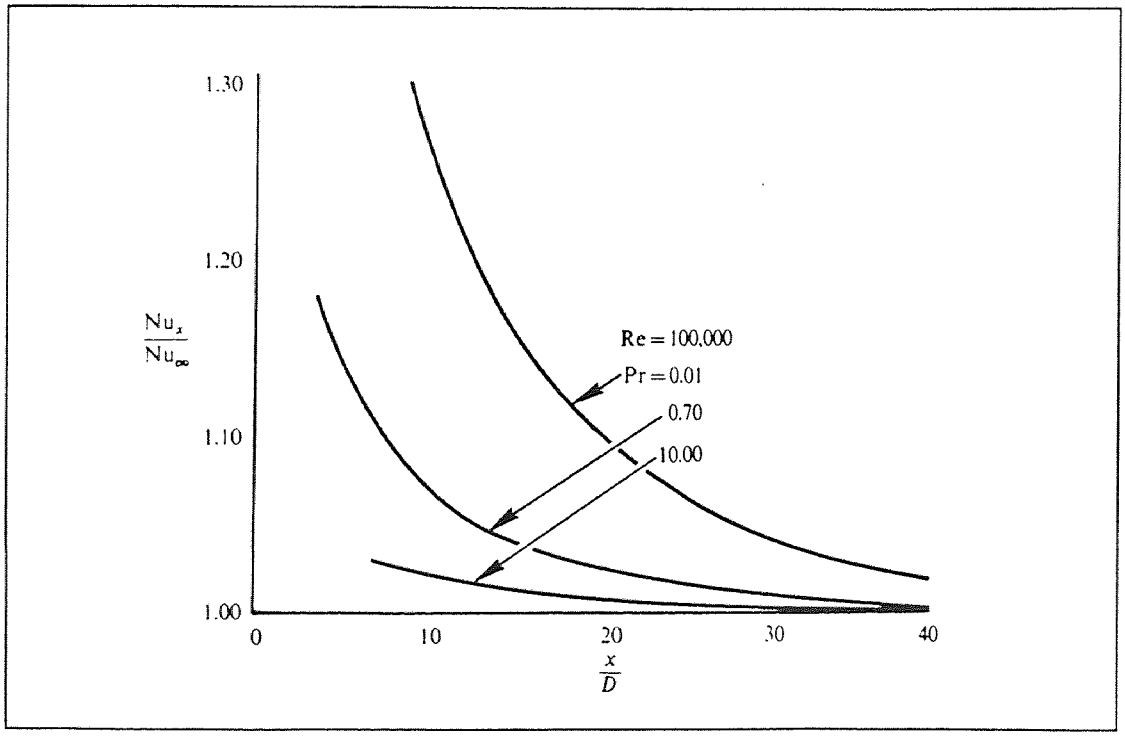

Figure 5.2 Variations of Turbulent Flow with Prandtl Numbers II

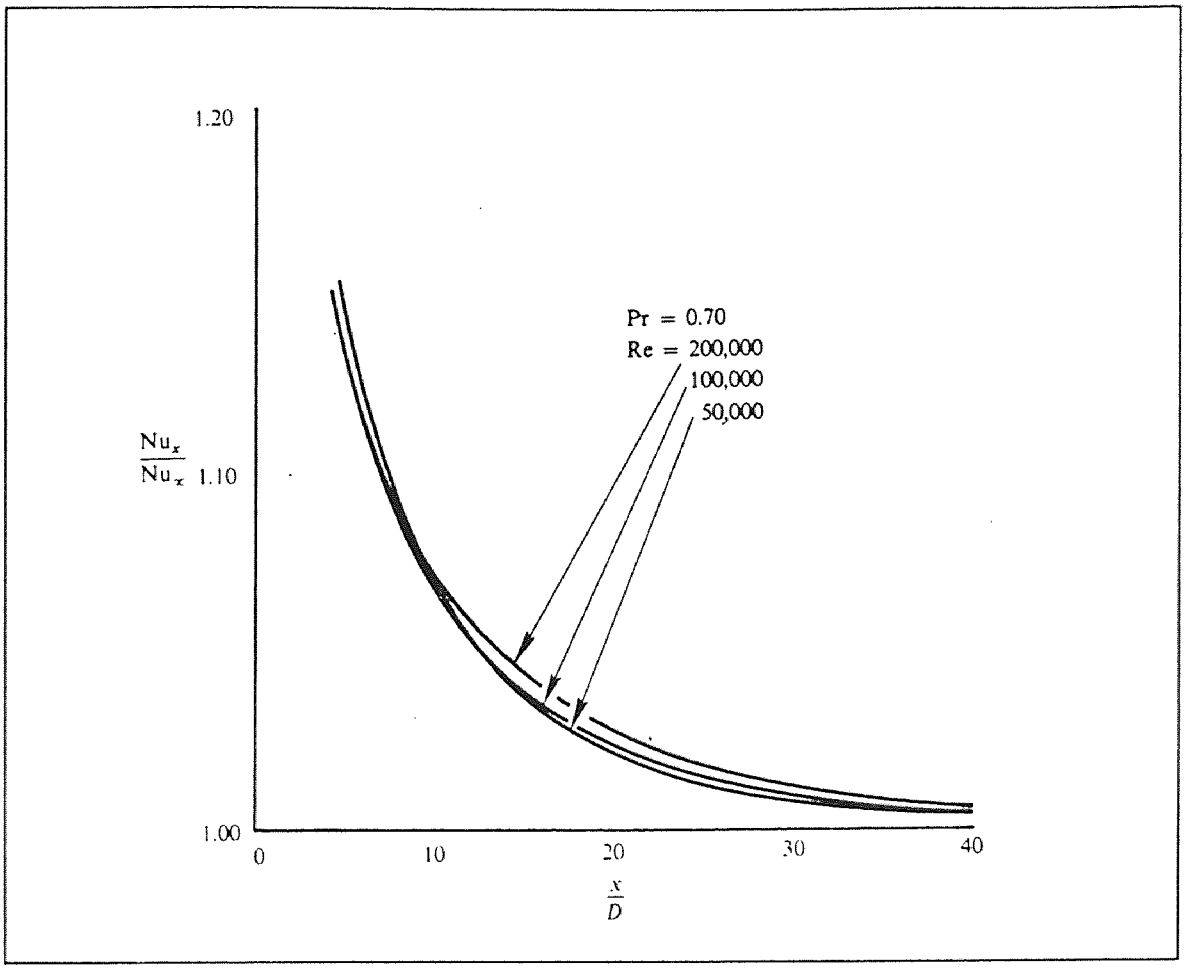

Figure 5.3 Variations of Turbulent Flow with Prandtl Number III

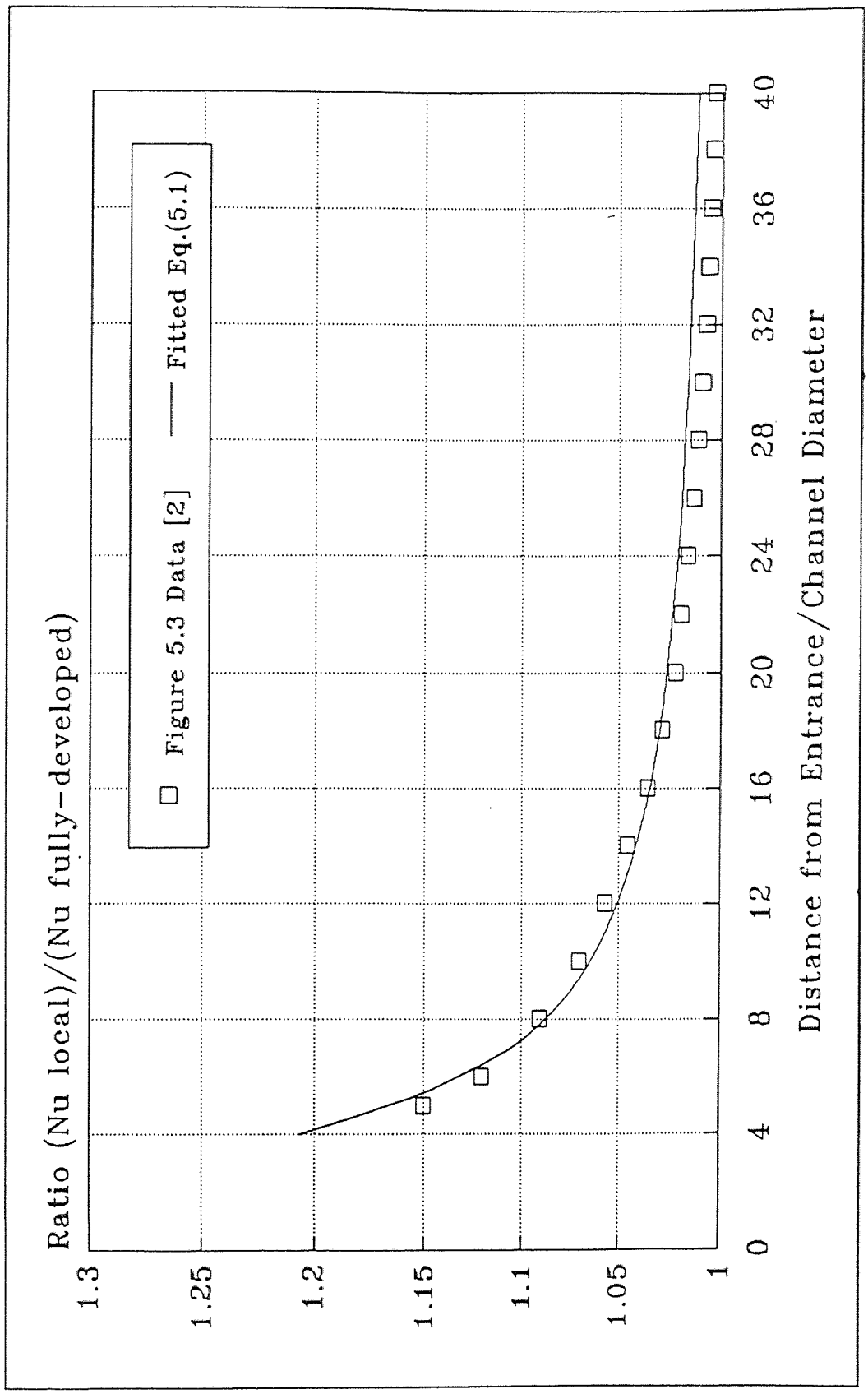

Figure 5.4 Local Nusselt Number in Channel Entry Region (Turbulent Flow)

CHAPTER SIX
SUMMARY AND CONCLUSIONS

It has been shown that for laminar flow in catalytic combustion reactors (Prandtl number near unity) the assumption of a fully developed flow (i.e., velocity, temperature, and concentration profiles are established) results in a substantial error in heat and mass transport evaluation. Effectively neglecting entry effects on heat and mass transfer result in underestimation of both heat transfer (Nusselt number) and mass transfer (Sherwood number). This work provides corrections to the transport correlations to account for these entry effects. Langhaar velocity profiles have been employed in numerical solutions for entry length heat transfer effects at constant wall temperature. Using the analogy between heat and mass transfer, similar solutions were written for entry length mass transfer effects. The numerical results were replaced by correlating equations for localized transport rates and inserted into a comprehensive computer based program which evaluates catalytic combustion reactors.

Using typical catalytic combustor conditions, the output of the model results in the following conclusions:

1. The reduced boundary layer thickness at the entrance to monolith channels results in catalytic "light-off" at lower inlet reactant temperatures, and a more rapid rise in overall fuel conversion as the inlet temperature is increased.

2. At the higher reactant inlet temperatures, the reduced boundary later thickness at the monolith entrance results in increased heat loss and subsequently in greatly diminished overall fuel conversion.

3. Catalytic combustion systems which use segmented bed reactors will be substantially affected by entry length conditions since each successive catalytic bed has the boundary layer restarted at the bed entrance.

Additional computations are recommended for the cases involving highly conductive beds and for entry length effects in turbulent flow. It is anticipated, in the latter case, that influence of entry effects on catalytic reactor performance will be considerably diminished.

APPENDIX
PROGRAM SOURCE FILE

The complete program source code consists of one main program and thirteen subroutines. Detailed description to be published elsewhere. The program blocks are listed as follows:

1. ABPARM compute uncorrelated dimensionless groups from physical input.
2. CATMAIN main program of the catalytic modeling.
3. DBVPFD IMSL routine to solve two-point boundary value problem.
4. DPLOTP IMSL routine to plot dimensionless output.
5. FCNBC calculated by DBVPFD provides boundary conditions.
6. FCNEQN calculated by DBVPFD provides differential equations.
7. FCNJAC calculated by DBVPFD provides Jacobian for solution technique.
8. LOSET analytical initial iterate assuming mass transport control.
9. MLCOR computer correlated dimensionless groups for monolith configuration.
10. OUTDIM prints solution table in dimensionless form.
11. OUTPHY prints solution table in physical or dimensional form.
12. PBCOR compute correlated dimensionless groups for packed bed configuration.
13. UNSET analytical initial iterate assuming no reaction.
14. UPSET analytical initial iterate assuming gas phase combustion.

As originally stated, the program calculates an average heat (and mass) transport coefficient over the length of the monolith. This average value is then applied as a constant value at every element along the catalyst

length. The program is now modified by the inclusion of a user suitable parameter designated as INLET. If INLET=1 then equation (3.13) substitutes for the heat transfer coefficient at every vector length (x/L). This change only affect the program handling of the equation set (subroutine FCNEQN) and the solution Jacobian (subroutine FCNJAC). Modified versions of these two routines are presented below. In the program, symbols dummy (18) and dummy (19) represent monolith bed length and channel diameter respectively. The modifications added to the program are highlighted in bold face print.

```
      SUBROUTINE  FCNEQN(NEQNS,X,Y,P,DYDX)

*     INVOKED BY DIFFERENTIAL EQUATION SOLVER (DBVPFD) TO
*     RETURN RHS OF FIRST ORDER DIFFERENTIAL EQS AS dY/dZ=F(Y,
*     DIM'LESS) AS A DYDX ARRAY DYDX(1)=dT/dZ, DYDX(2)=dV/dZ,
*     DYDX(3)=dTs/dZ, DYDX(4)=dW1/dZ, DYDX(5)=dW2/dZ: DD 10/92

      IMPLICIT REAL*8(A-H,O-Z)
      DIMENSION Y(NEQNS),DYDX(NEQNS),GC(2),BPAR(2),DAC(2),
     & GH(2),DAH(2),AANF(2),AANO(2),PHI(2),W(2),R(2),WV(2),
     & PWV(2),AAJD(2)
      COMMON/PARM/GC1,BPAR1,DAC1,AJD,AJE,AJH,AJF,PES,GH1,
     & DAH1,AANF1,AANO1,PHI1,DUMMY(24),NSPEC
      COMMON/PARM0/GC2,BPAR2,DAC2,AANF2,AANO2,PHI2,GH2,DAH2,
     & AJD2
      COMMON /PARM3/GC,BPAR,DAC,AANF,AANO,PHI,GH,DAH
      COMMON/FINLET/INLET,PR,CCFAC,REYN,SCMEAN1,SCMEAN2
*     ACCOUNT FOR INLET BL EFFECTS (INLET=1): LAMINAR FLOW
      IF (INLET.EQ.1) THEN
      IF (X.EQ.0.0) THEN
      AJH=100.0
      AJD=100.0
      IF (NSPEC.EQ.2) AJD2=100.0
      ELSE
      AK=PR*REYN*DUMMY(19)/(X*DUMMY(18))
      IF (REYN.GT.2300.0) THEN
      TNUXF=1.0D0+(1.338D0*(DUMMY(19)/X*DUMMY(18))**1.3D0)/
     & ((1.0D0+3.271D2*(DUMMY(19)/X*DUMMY(18))
     & **0.1D0)**2.5D0)
      TNUF=2.3D-2*PR**0.5D0*REYN**0.8D0
      ANU=TNUXF*TNUF
      ELSE
      ANU=3.66D0+(1.33D-3*AK**1.8D0)/(1.0D0+1.6D-
     & 2*AK**0.8D0)**2.0D0
      ENDIF
      AJH=4.0D0*ANU/AK
      AJD=(AJH/CCFAC)*(PR/SCMEAN1)**0.667D0
      IF (NSPEC.EQ.2) AJD2=(AJH/CCFAC)*(PR/SCMEAN2)**0.667D0
      ENDIF
      ENDIF
      J=NSPEC
      NB=NSPEC+3
      W(1)=Y(4)
      V=Y(2)
      WV(1)=W(1)/V
      GC(1)=GC1
      BPAR(1)=BPAR1
      DAC(1)=DAC1
      AANF(1)=AANF1
      AANO(1)=AANO1
```

```
      PHI(1)=PHI1
      GH(1)=GH1
      DAH(1)=DAH1
      AAJD(1)=AJD
      IF (NSPEC.EQ.2) THEN
      W(2)=Y(5)
      WV(2)=W(2)/V
      GC(2)=GC2
      BPAR(2)=BPAR2
      DAC(2)=DAC2
      AANF(2)=AANF2
      AANO(2)=AANO2
      PHI(2)=PHI2
      GH(2)=GH2
      DAH(2)=DAH2
      AAJD(2)=AJD2
      ENDIF
*   COMPUTE ([O2]/[O2]o)**m = (Cz/Czo)**m
      PREWV=1.D0
      DO 10 I=1,J
      PREWV=(W(I)-1.D0)*PHI(I)+PREWV
10    CONTINUE
      DO 20 I=1,J
      PWV(I)=(PREWV/V)**AANO(I)
20    CONTINUE
*   COMPUTE NON-SUMMATION TERMS
      DYDX(1)=AJH*(Y(3)-Y(1))
      DYDX(3)=PES*Y(1)
*   COMPUTE SUMMATION TERMS d/dZ for T, Ts, W1, W2
      DO 30 I=1,J
      R(I)=DAC(I)/AAJD(I)
      EXPT=Y(1)/(Y(1)+1.D0)*GH(I)
      EXPTS=-Y(3)/(Y(3)+1.D0)*GC(I)
      REXPT=1.D0/(R(I)+DEXP(EXPTS))
      AD=WV(I)**AANF(I)
      DYDX(1)=DYDX(1)+BPAR(I)*DAH(I)*WV(I)**AANF(I)*PWV(I)
     & *DEXP(EXPT)
      DYDX(3)=PES*BPAR(I)*(W(I)-1.D0)+DYDX(3)
      DYDX(3+I)=-DAC(I)*WV(I)*REXPT-
DAH(I)*WV(I)**AANF(I)*PWV(I)
     & *DEXP(EXPT)
30    CONTINUE
*   COMPUTE d/dZ FOR V
      ANUM1=AJE*Y(2)*DYDX(1)+AJF*Y(2)**3
      DEN1=AJE*(Y(1)+1.D0)-Y(2)*Y(2)
      DYDX(2)=ANUM1/DEN1
      RETURN
      END
```

```
      SUBROUTINE FCNJAC(NEQNS,X,Y,P,DYPDY)

*     INVOKED BY DIFFERENTIAL EQUATION SOLVER (DBVPFD) TO
*     COMPUTE THE JACOBIAN OF THE FUNCTIONS EVALUATED IN
*     FCNEQN VALUES RETURNED IN TWO-D ARRAY DYPDY(X,Y) WHERE X
*     IS THE FIRST DERIVATIVE OR DIFF EQ FOR VARIABLE X AND Y
*     IS THE DERIVATIVE OF THIS EQUATION WITH RESPECT TO
*     VARIABLE Y): DD 10/92

      IMPLICIT REAL*8 (A-H,O-Z)
      DIMENSION Y(NEQNS),DYPDY(NEQNS,NEQNS),GC(2),BPAR(2),
     & DAC(2),AANF(2),AANO(2),PHI(2),GH(2),DAH(2),W(2),
     & WV(2),R(2),R1(2),EEEXPT(2),EXPTS(2),PWV(2),WVNF1(2),
     & WVNF(2),PWVN1(2),PWVN(2)
      COMMON/PARM/GC1,BPAR1,DAC1,AJD,AJE,AJH,AJF,PES,GH1,
     & DAH1,AANF,AANO1,PHI1,DUMMY(24),NSPEC
      COMMON /PARM0/GC2,BPAR2,DAC2,AANF2,AANO2,PHI2,GH2,
     & DAH2,AJD2
      COMMON/PARM3/GC,BPAR,DAC ,AANF,AANO,PHI,GH,DAH
      COMMON/FINLET/INLET,PR,CCFAC,REYN,SCMEAN1,SCMEAN2
*     ACCOUNT FOR INLET BL EFFECTS (INLET=1): LAMINAR FLOW
      IF (INLET.EQ.1) THEN
      IF (X.EQ.0.0) THEN
      AJH=100.0
      AJD=100.0
      IF (NSPEC.EQ.2) AJD2=100.0
      ELSE
      AK=PR*REYN*DUMMY(19)/(X*DUMMY(18))
      IF (REYN.GT.2300.0) THEN
      TNUXF=1.0D0+(1.338D0*(DUMMY(19)/X*DUMMY(18))**1.3D0)/
     & ((1.0D0+3.271D2*(DUMMY(19)/X*DUMMY(18))
     & **0.1D0)**2.5D0)
      TNUF=2.3D-2*PR**0.5D0*REYN**0.8D0
      ANU=TNUXF*TNUF
      ELSE
      ANU=3.66D0+(1.33D-3*AK**1.8D0)/(1.0D0+1.6D-
     & 2*AK**0.8D0)**2.0D0
      ENDIF
      AJH=4.0D0*ANU/AK
      AJD=(AJH/CCFAC)*(PR/SCMEAN1)**0.667D0
      IF (NSPEC.EQ.2) AJD2=(AJH/CCFAC)*(PR/SCMEAN2)**0.667D0
      ENDIF
      ENDIF
      J=NSPEC
      T=Y(1)
      V=Y(2)
      TS=Y(3)
      W(1)=Y(4)
      WV(1)=W(1)/V
      IF (NSPEC.EQ.2) THEN
```

```
      W(2)=Y(5)
      WV(2)=W(2)/V
      ENDIF
*   (1+T)
      T1=Y(1)+1.D0
*   1/(1+T)
      T11=1.D0/T1
*   EXP[1/(1+T)]
      DD=DEXP(T11)
*   1/(1+T)^2
      T12=T11*T11
*   (1+Ts)
      TS1=Y(3)+1.D0
*   1/(1+Ts)
      TS11=1.D0/TS1
*   1/(1+Ts)^2
      TS12=TS11*TS11
*   T/(1+T)
      EXPT1=Y(1)*T11
*   Ts/(1+Ts)
      EXPTS1=Y(3)*TS11
*   GAMMAg1[T/(1+T)]
      EXPT10=EXPT1*GH(1)
*   GAMMAg2[T/(1+T)]
      EXPT20=EXPT1*GH(2)
*   1+SUMMATION(Wi-1)PHIi = (Cz/Czo)V
      PREPWV=1.D0
      DO 10 I=1,J
      PREPWV=PHI(I)*W(I)-PHI(I)+PREPWV
10    CONTINUE
*   AJH(Ts-T)
      DYDX1=AJH*(Y(3)-Y(1))
      DO 20 I=1,J
*   GAMMAgi[T/(1+T)]
      EEEXPT(I)=EXPT1*GH(I)
*   (Wi/V)^ni AND (Wi/V)^(ni-1)
      WVNF(I)=WV(I)**AANF(I)
      WVNF1(I)=WV(I)**(AANF(I)-1.D0)
*   (Cz/Czo)^(ni-1) AND (Cz/Czo)^ni
      PWVN1(I)=(PREPWV/V)**(AANO(I)-1.D0)
      PWVN(I)=PWVN1(I)*(PREPWV/V)
*   dT/dZ
      DYDX1=DYDX1+BPAR(I)*DAH(I)*WVNF(I)*PWVN(I)
     & *DEXP(EEEXPT(I))
20    CONTINUE
*   V^2
      V2=V*V
*   1/V
      RV=1.D0/V
*   1/V^2
      RV2=RV*RV
```

```
*    1/V
       PWV1=RV
       ANUM=AJE*V*DYDX1+AJF*V*V2
       RDEN=1.D0/(AJE*T1-V2)
       RDEN2=RDEN*RDEN
       DYPDY(1,1)=-AJH
       DYPDY(1,2)=0.D0
       DYPDY(1,4)=BPAR(1)*DAH(1)*WVNF1(1)*PWVN(1)
      & *DEXP(EXPT10)*AANF(1)*RV
       PREDY=0.0D0
       IF (NSPEC.EQ.2) DYPDY(1,5)=BPAR(2)*DAH(2)*WVNF1(2)
      & *PWVN(2)*DEXP(EXPT20)*AANF(2)*RV
       DO 30 I=1,J
*    GAMMAgi[T/(1+T)]
       EEEXPT(I)=EXPT1*GH(I)
*    GAMMAsi[Ts/(1+Ts)]
       EXPTS(I)=EXPTS1*(-GC(I))
*    ri
       R(I)=DAC(I)/AJD
*    1/(ri+EXP(-GAMMAsi[Ts/(1+Ts)]))
       R1(I)=1.D0/(R(I)+DEXP(EXPTS(I)))
       DYPDY(1,1)=DYPDY(1,1)+BPAR(I)*DAH(I)*WVNF(I)
      & *PWVN(I)*DEXP(EEEXPT(I))*GH(I)*T12
       DYPDY(1,2)=DYPDY(1,2)-BPAR(I)*DAH(I)*WVNF(I)*PWVN(I)
      & *DEXP(EEEXPT(I))*RV*(AANF(I)+AANO(I))
       PREDY=BPAR(I)*DAH(I)*WVNF(I)*PWVN1(I)*
      & DEXP(EEEXPT(I))*AANO(I)*RV+PREDY
       DYPDY(3+I,1)=-DAH(I)*WVNF(I)*PWVN(I)*DEXP(EEEXPT(I))
      & *GH(I)*T12
       DYPDY(3+I,2)=DAC(I)*W(I)*RV2*R1(I)+DAH(I)
      & *DEXP(EEEXPT(I))
      & *WVNF(I)*PWVN(I)*(AANF(I)+AANO(I))*RV
       DYPDY(3+I,3)=-DAC(I)*WV(I)*GC(I)*DEXP(EXPTS(I))
      & *TS12*R1(I)*R1(I)
30     CONTINUE
       DYPDY(1,3)=AJH
       DYPDY(1,4)=PREDY*PHI(1)+DYPDY(1,4)
       DYPDY(2,1)=AJE*V*DYPDY(1,1)*RDEN-AJE*ANUM*RDEN2
       ANM22=AJE*DYDX1+AJE*V*DYPDY(1,2)+3.D0*AJF*V2
       DYPDY(2,2)=ANM22*RDEN+2.D0*V*ANUM*RDEN2
       DYPDY(2,3)=AJH*RDEN*AJE*V
       DYPDY(2,4)=AJE*DYPDY(1,4)*RDEN*V
       IF (NSPEC.EQ.2) THEN
       DYPDY(1,5)=PREDY*PHI(2)+DYPDY(1,5)
       DYPDY(2,5)=AJE*DYPDY(1,5)*REDN*V
       DYPDY(3,5)=PES*BPAR(2)
       ENDIF
       DYPDY(3,1)=PES
       DYPDY(3,2)=0.D0
       DYPDY(3,3)=0.D0
       DYPDY(3,4)=PES*BPAR(1)
```

```
 DYPDY(4,4)=-DAC(1)*RV*R1(1)-DAH(1)*WVNF1(1)*PWVN1(1)
&  *RV*DEXP(EEEXPT(1))*(AANF(1)*PREPWV*RV+WV(1)
*  *AANO(1)*PHI(1))
 IF(NSPEC.EQ.2)  DYPDY(4,5)=-DAH(1)*WVNF(1)
&  *PWVN1(1)*DEXP(EEEXPT(1))*AANO(1)*RV*PHI(2)
 IF  (NSPEC.EQ.2)  THEN
 DYPDY(5,4)=-DAH(2)*WVNF(2)*PWVN1(2)
&  *DEXP(EEEXPT(2))*RV*PHI(1)*AANO(2)
 DYPDY(5,5)=-DAC(2)*RV*R1(2)-DAH(2)*WVNF1(2)
&  *PWVN1(2)*RV*DEXP(EEEXPT(2))*(AANF(2)*PREPWV*RV
&  +AANO(2)*PHI(2)*WV(2))
 ENDIF
 RETURN
 END
```

REFERENCES

[1] Cerkanowicz, A. E., R. B. Cole, and J. G. Stevens. "Catalytic Combustion Modeling; Comparison with Experimental Data." *Transaction of the ASME*, 99, Series A, No. 4, (1977): 593-600.

[2] Kays, W. M. "Numerical Solution for Laminar Flow Heat Transfer in Circular Tubes." *Transaction of the ASME,* 77 (1955): 1265-1274.

[3] Kays, W. M. and M. E. Crawford. *Convective Heat and Mass Transfer*. 2nd ed., New York: McGraw-Hill 1980.

[4] Shah, R. K. and A. L. London. *Laminar Flow Forced Convection in Ducts*. New York: Academic Press 1978.

[5] White, F. M. *Heat and Mass Transfer*. New York: Addison-Wesley 1988.

[6] Spalding, D. B. *Convective Mass Transfer*. London: Edward Arnold Ltd. 1963.

[7] Yang, Jing. "Modeling Packed Bed Catalytic Reactors." Thesis-Master of Science in Mechanical Engineering, (1990), Dr. A. E. Cerkanowicz: Advisor.

[8] Eckert, R. G. *Introduction to the Transfer of Heat and Mass*. New York: McGraw-Hill Book Company, Inc. 1950.

[9] Langhaar, H. L. "Steady Flow in the Transition Length of a Straight Tube." *Journal of Applied Mechanics,* Trans. ASME, 64 (1942): A-55.

[10] Kreith, Frank, and Mark S. Bohn. *Principles of Heat Transfer*. 4th. ed., New York: Harper & Row, Publishers, Inc. 1986.

[11] Thomas, Lindon C. *Heat Transfer*. New Jersey: Prentice-Hall, Inc. 1991.

[12] Satterfield, Charles N. *Mass Transfer In Heterogeneous Catalysis*. Massachusetts Institute of Technology, Massachusetts, 1977.